Electronic Supplementary Information

Two carbazole disulfonamide-diamide macrocycles with the semi-flexible *meta*-xylyl linkages for anion recognition

Junhong Li,[a] Lisha Yuan,[a] Qinrong Yang,[a] Ningjin Zhang,*[b] and Xiaoping Bao*[a]

[a] *Center for Research and Development of Fine Chemicals, State Key Laboratory Breeding Base of Green Pesticide and Agricultural Bioengineering, Key Laboratory of Green Pesticide and Agricultural Bioengineering, Ministry of Education, Guizhou University, Guiyang 550025*
E-mail: baoxp_1980@aliyun.com
[b] *Instrumental Analysis Center, Shanghai Jiaotong University, Shanghai 200240, China. E-mail: hannahznj@sjtu.edu.cn*

Contents

Experimental

Materials and general methods

All the chemicals were purchased from commercial suppliers and used without further purification (unless stated otherwise). All the anions were added as their tetra-*n*-butylammonium (TBA) salts. Melting points were measured on a SGW X-4 micro-melting point apparatus and uncorrected. All the ^{1}H and ^{13}C NMR data were collected on a JEOL-ECX 500 NMR spectrometer and calibrated to the residual solvent peak in DMSO-d_6 (D, 99.8%) at 298 K, and chemical shift (δ) was expressed in parts per million (ppm). The following abbreviations were utilized in expressing the multiplicity: s = singlet, d = doublet, t = triplet, q = quartet, m = multiplet. High resolution mass spectra (HRMS) were recorded on a Thermo Scientific Q Exactive Hybrid Quadrupole-Orbitrap mass spectrometer. The X-ray crystallographic data were gathered using a Bruker D8 Venture diffractometer. UV-vis spectra were collected on a Beijing PGENERAL TU-1900 spectrometer. All the non-linear curve fitting analyses were conducted using the software of Origin 6.0.

Synthesis

Synthesis of bis-amine 4

Carbazole-1,8-disulfonyl chloride **5** (1.00 g, 2.10 mmol) dissolved in dichloromethane (50 mL) was added dropwise to a dichloromethane solution (50 mL) containing 1,3-bis(aminomethyl)benzene (2.77 mL, 21.00 mmol), and the reaction mixture was stirred at room temperature for 8 h. After the reaction was completed, the reaction solution was concentrated and then purified by flash column chromatography on silica gel (DCM/EtOH = 40:1 (*v*/*v*) as an eluent) to afford bis-amine **4** (0.30 g, 21% yield): mp 162–163 °C; ^{1}H NMR (500 MHz, DMSO-d_6) δ: 8.61 (s, 2H), 7.83 (s, 2H), 7.08–7.05 (m, 6H), 6.98 (d, J = 5.0 Hz, 2H), 4.04 (s, 4H), 3.49 (s, 4H), 1.41 (s, 18H); ^{13}C NMR (125 MHz, DMSO-d_6) δ: 143.9, 142.7, 136.8, 133.8, 127.9, 126.1, 125.8, 125.4, 124.1, 122.7, 122.3, 121.9, 46.3, 45.4, 34.8, 31.6; HRMS (ESI) *m*/*z*: $[M + H]^+$ calcd for $C_{36}H_{46}N_5O_4S_2$: 676.2986, found: 676.2991.

Synthesis of macrocycle 1

A dry CH_2Cl_2 solution (50 mL) containing 2,6-pyridinedicarbonyl dichloride (0.42 g, 2.03 mmol) was slowly added to a CH_2Cl_2 solution containing bis-amine **4** (1.10 g, 1.63 mmol) and dry TEA (2.26 mL, 16.27 mmol), and the above solution was stirred at room temperature for 3 h. After the reaction was completed, the solvent was removed under reduced pressure and the resultant mixture was purified by flash column chromatography on silica gel (CH_2Cl_2/CH_3CN = 4:1 (*v*/*v*) as an eluent) to give pure macrocycle **1** (0.25 g, 19%): mp 271–273 °C; ^{1}H NMR (500 MHz, DMSO-d_6) δ: 10.25 (s, 1H), 9.74 (t, J = 10.0 Hz, 2H), 8.68 (d, J = 2.3 Hz, 2H), 8.49 (t, J = 7.5 Hz, 2H), 8.18–8.16 (m, 2H), 8.14–8.10 (m, 1H), 7.91 (d, J = 2.1 Hz, 2H), 7.31–7.24 (m, 6H), 7.03 (s, 2H), 4.52 (d, J = 5.0 Hz, 4H), 3.96 (d, J = 10.0 Hz, 4H), 1.43 (s, 18H); ^{13}C NMR (125 MHz, DMSO-d_6) δ: 163.3, 148.6, 143.0, 139.5, 139.4, 138.0, 133.9, 128.6, 126.9, 125.9, 125.6, 124.5, 124.2, 122.8, 122.6, 121.6, 45.8, 42.0, 34.9, 31.6; HRMS (ESI) *m*/*z*: $[M + Na]^+$ calcd for $C_{43}H_{46}N_6NaO_6S_2$: 829.2812, found: 829.2804.

Synthesis of macrocycle 2

Macrocycle **2** was prepared in a similar manner to macrocycle **1**, using isophthaloyl dichloride as the acylating agent. 16% yield, mp >250 °C; ^{1}H NMR (500 MHz, DMSO-d_6) δ: 10.29 (s, 1H), 9.02 (t, J = 7.5 Hz, 2H), 8.70 (d, J = 2.3 Hz, 2H), 8.53 (s, 2H), 8.25 (s, 1H), 7.96 (d, J = 10.0 Hz, 2H), 7.92 (d, J = 2.0 Hz, 2H), 7.54 (t, J = 10.0 Hz, 1H), 7.29–7.17 (m, 8H), 4.40 (d, J = 5.0 Hz, 4H), 3.97 (d, J = 5.0 Hz, 4H), 1.44 (s, 18H); ^{13}C NMR (125 MHz, DMSO-d_6) δ: 165.7, 143.0, 142.5, 139.8, 137.9, 134.5, 133.9, 130.1, 128.7, 128.3, 127.3, 126.4, 126.1, 124.3, 122.8, 122.6, 121.7, 46.1, 42.7, 34.9, 31.7; HRMS (ESI) *m*/*z*: $[M - H]^-$ calcd for $C_{44}H_{46}N_5O_6S_2$: 804.2884, found: 804.2903.

Synthesis of acyclic receptor 3

A solution of bis-amine **4** (0.35 g, 0.52 mmol), butyryl chloride (0.13 g, 1.19 mmol), and dry TEA (0.72 mL, 5.18 mmol) in dry CH_2Cl_2 (70 mL) was stirred at room temperature overnight. After the reaction was completed, the solvent was removed under reduced pressure and the resulted mixture was purified by column chromatography over silica gel (CH_2Cl_2/MeOH = 50:1 (*v*/*v*) as an eluent) to afford pure

receptor **3** (0.12 g, 29% yield): mp 140–143 °C; ^{1}H NMR (500 MHz, DMSO-d_6) δ: 10.30 (s, 1H), 8.63 (d, J = 2.4 Hz, 2H), 8.56 (t, J = 7.5 Hz, 2H), 8.16 (t, J = 7.5 Hz, 2H), 7.85 (d, J = 2.2 Hz, 2H), 7.11–7.08 (m, 2H), 7.01–6.98 (m, 6H), 4.06 (d, J = 10.0 Hz, 4H), 4.02 (d, J = 10.0 Hz, 4H), 2.05 (t, J = 10.0 Hz, 4H), 1.54–1.45 (m, 4H), 1.42 (s, 18H), 0.82 (t, J = 10.0 Hz, 6H); ^{13}C NMR (125 MHz, DMSO-d_6) δ: 172.0, 142.9, 139.8, 137.2, 133.8, 128.2, 126.4, 126.1, 125.9, 124.2, 122.8, 122.5, 121.8, 46.2, 41.8, 37.3, 34.8, 31.7, 18.8, 13.7; HRMS (ESI) m/z: $[M + H]^+$ calcd for $C_{44}H_{58}N_5O_6S_2$: 816.3823, found: 816.3815.

^{1}H NMR titrations

^{1}H NMR titration experiments were carried out on a JEOL-ECX 500 NMR spectrometer and calibrated to the residual solvent peak in DMSO-d_6 (D, 99.8%) at 298 K. In all cases, the ^{1}H NMR titrations were conducted while keeping the concentration of receptor compounds (1.0 mM in DMSO-d_6) constant *via* dissolving guest anions with the same receptor solution to prepare guest solution. The anion solution was directly added to 0.5 mL solution of the receptor using an appropriate pipette, and the resultant NMR spectra were recorded after each addition of the anions. The aforementioned operations ensured that the concentration of the receptors remained unchanged, whereas the concentration of the added anions varied continuously. Finally, the chemical shifts of the specific proton were plotted against the number of equivalents of the added anions and the binding constant (K) was determined assuming a 1:1 binding model, using the following equation:[1,2]

$$\delta = \delta_0 + (\delta_{lim}-\delta_0)/2C_0 \{(C_0 + C_G + 1/K)-[(C_0 + C_G + 1/K)^2 -4C_0C_G]^{1/2}\}$$

Where C_0 and C_G are the corresponding concentrations of the host and guest anion; δ and δ_0 represent the chemical shift of the host in the presence or absence of guest anions, respectively. Considering "$(\delta_{lim}-\delta_0)/C_0$" being a definite value, the letter of "a" was employed to substitute this mathematical expression during the actual nonlinear fitting process for convenience.

UV-vis titrations

UV-vis titration experiments were conducted on a TU-1900 UV-visible spectrophotometer, by adding a DMSO (99.8% purity) solution containing fluoride ion (5.0 mM) into the receptor (20 μM in DMSO) at 298 K. The resulting absorption spectra were recorded after each addition. For a complex with a 1:1 binding stoichiometry, the binding constant (*K*) can be determined based on the following equation:[3,4]

$$A = A_0 + (A_{lim}-A_0)/2C_0 \{(C_0 + C_G + 1/K)-[(C_0 + C_G + 1/K)^2 -4C_0C_G]^{1/2}\}$$

Where A and A_0 represent the absorbances of the host in the presence or absence of guest anion, respectively; C_0 and C_G are the corresponding concentration of the host and guest anion. Considering "$(A_{lim}-A_0)/C_0$" being a definite value, the letter of "a" (shown in the fitting graphs) was employed to substitute this mathematical expression during the actual nonlinear fitting process for convenience.

References

1 A. Szumna and J. Jurczak, A New Macrocyclic Polylactam-Type Neutral Receptor for Anions–Structural Aspects of Anion Recognition, *Eur. J. Org. Chem.*, 2001, 4031–4039.

2 A. Sumida, R. Kobayashi, T. Yumura, H. Imoto and K. Naka, Dibenzoarsacrowns: an experimental and computational study on the coordination behaviors, *Chem. Commun.*, 2021, **57**, 2013–2016.

3 J. Bourson, J. Pouget and B. Valeur, Ion-Responsive Fluorescent Compounds. **4**. Effect of Cation Binding on the Photophysical Properties of a Coumarin Linked to Monoaza- and Diaza-Crown Ethers, *J. Phys. Chem.*, 1993, **97**, 4552–4557.

4 G. Y. Qing, Y. B. He, Y. Zhao, C. G. Hu, S. Y. Liu and X. Yang, Calix[4]arene-Based Chromogenic Chemosensor for the α-Phenylglycine Anion: Synthesis and Chiral Recognition, *Eur. J. Org. Chem.*, 2006, 1574–1580.

^{1}H NMR titrations

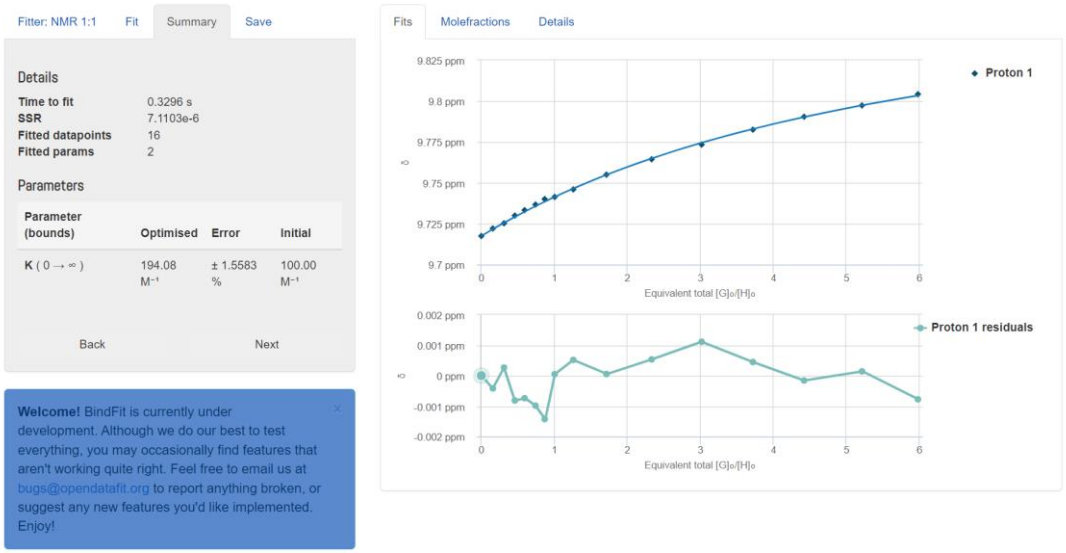

Fig. S1 The corresponding isotherm of macrocycle **1** with ^{n}Bu$_4$NAcO based on a 1:1 model using the www.supramolecular.org web applet, giving K_a = 194 M^{-1}. The monitored signal was corresponding to amide NH protons. The residual distribution was displayed below the binding isotherm.

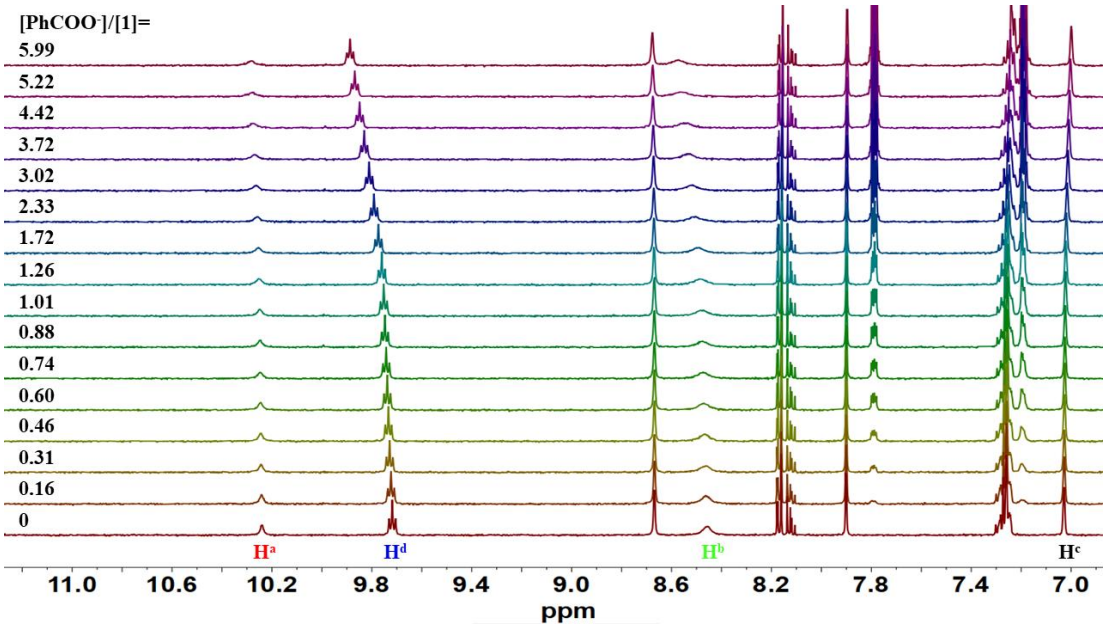

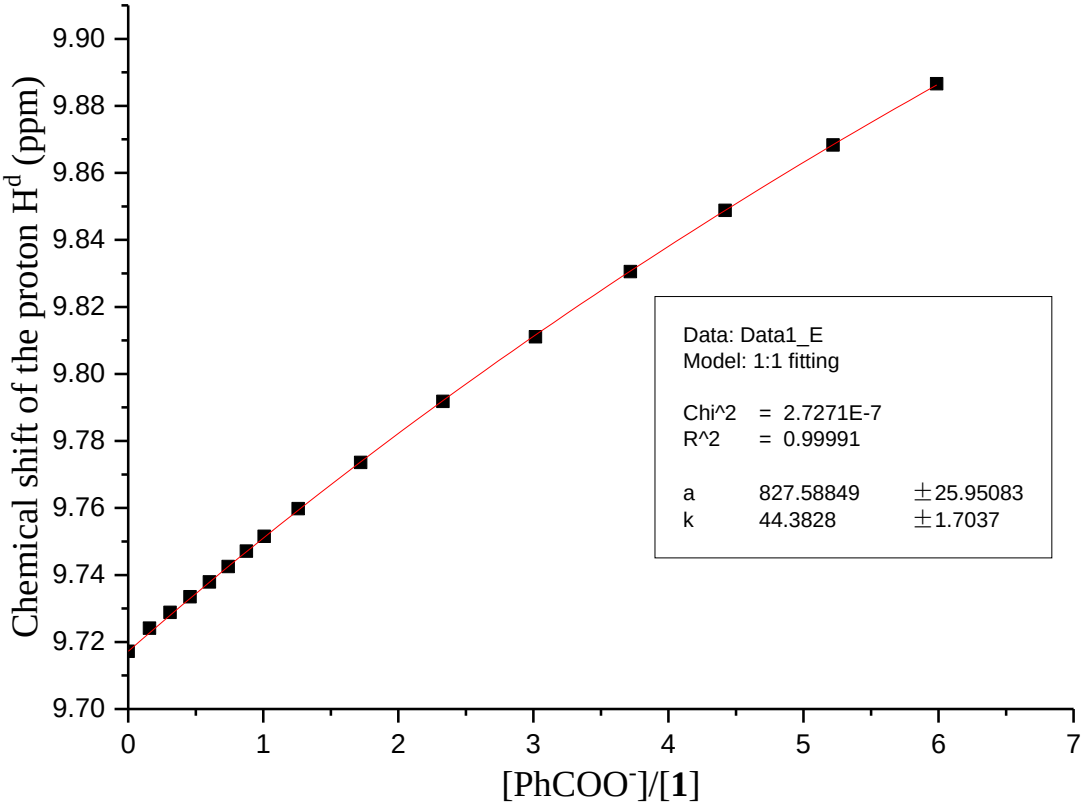

Fig. S2 Top: Stack plot of ^{1}H NMR titration of macrocycle **1** (1.0 mM) with ^{n}Bu$_4$NPhCOO in DMSO-d_6 at 298 K. Bottom: The non-linear curve fitting of the chemical shifts for amide NH signals (H^d) in macrocycle **1** against equivalents of PhCOO$^-$, assuming a 1:1 binding model.

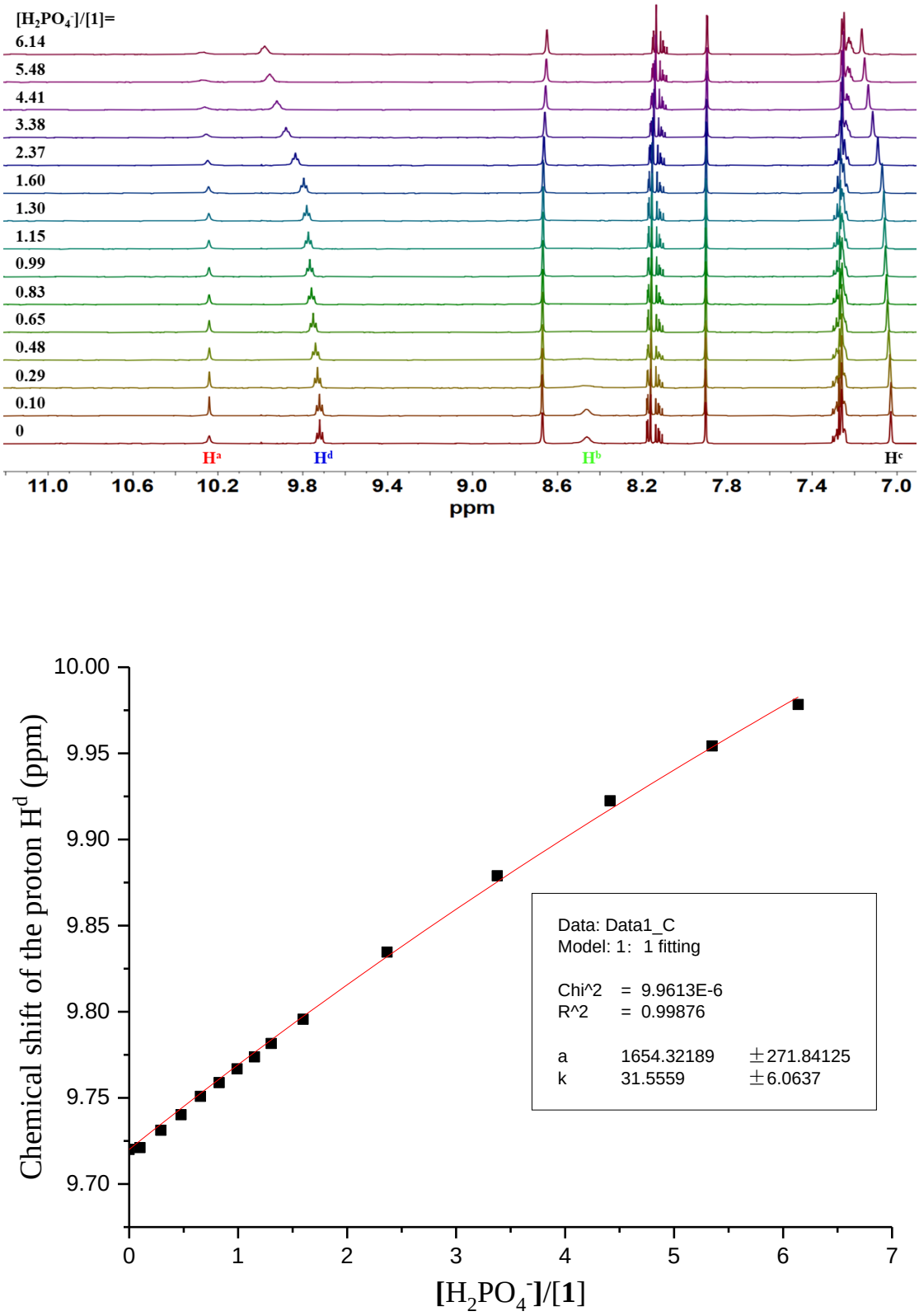

Fig. S3 Top: Stack plot of ^{1}H NMR titration of macrocycle **1** (1.0 mM) with ^{n}Bu$_4$NH$_2$PO$_4$ in DMSO-d_6 at 298 K. Bottom: The non-linear curve fitting of the chemical shifts for amide NHs signal (H^d) in macrocycle **1** against equivalents of $H_2PO_4^-$, using a 1:1 binding model.

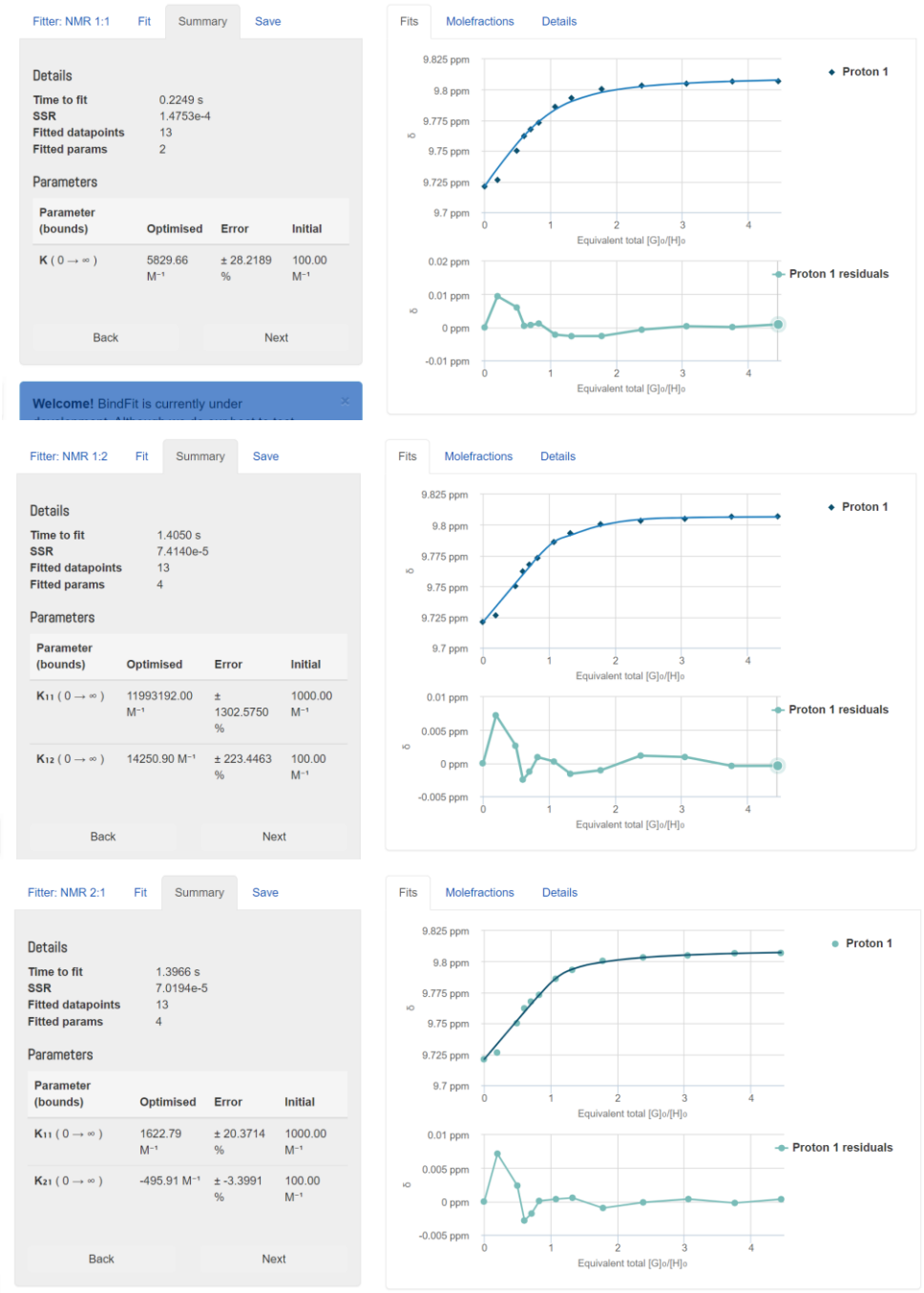

Fig. S4 Top: The corresponding isotherm of macrocycle **1** with ^{n}Bu$_4$NF based on a 1:1 model using the www.supramolecular.org web applet, giving K_a = 5830 M^{-1}. The monitored signal was amide NH protons. The residual distribution was displayed below the binding isotherm. Middle: The corresponding isotherm of macrocycle **1** with ^{n}Bu$_4$NF based on a 1:2 model using the www.supramolecular.org web applet, giving K_{11} = 11993192 M^{-1} and K_{12} = 14251 M^{-1}. The monitored signal was amide NH protons. The residual distribution was displayed below the binding isotherm. Bottom: The corresponding isotherm of macrocycle **1** with ^{n}Bu$_4$NF based on a 2:1 model using the www.supramolecular.org web applet, giving K_{11} = 1623 M^{-1} and K_{21} = –496 M^{-1}. The monitored signal was amide NH protons. The residual distribution was displayed below the binding isotherm. Considering the errors and negative values in the calculation of binding constants using the 1:2 and 2:1 models, the use of a 1:1 model was the most reasonable and reliable.

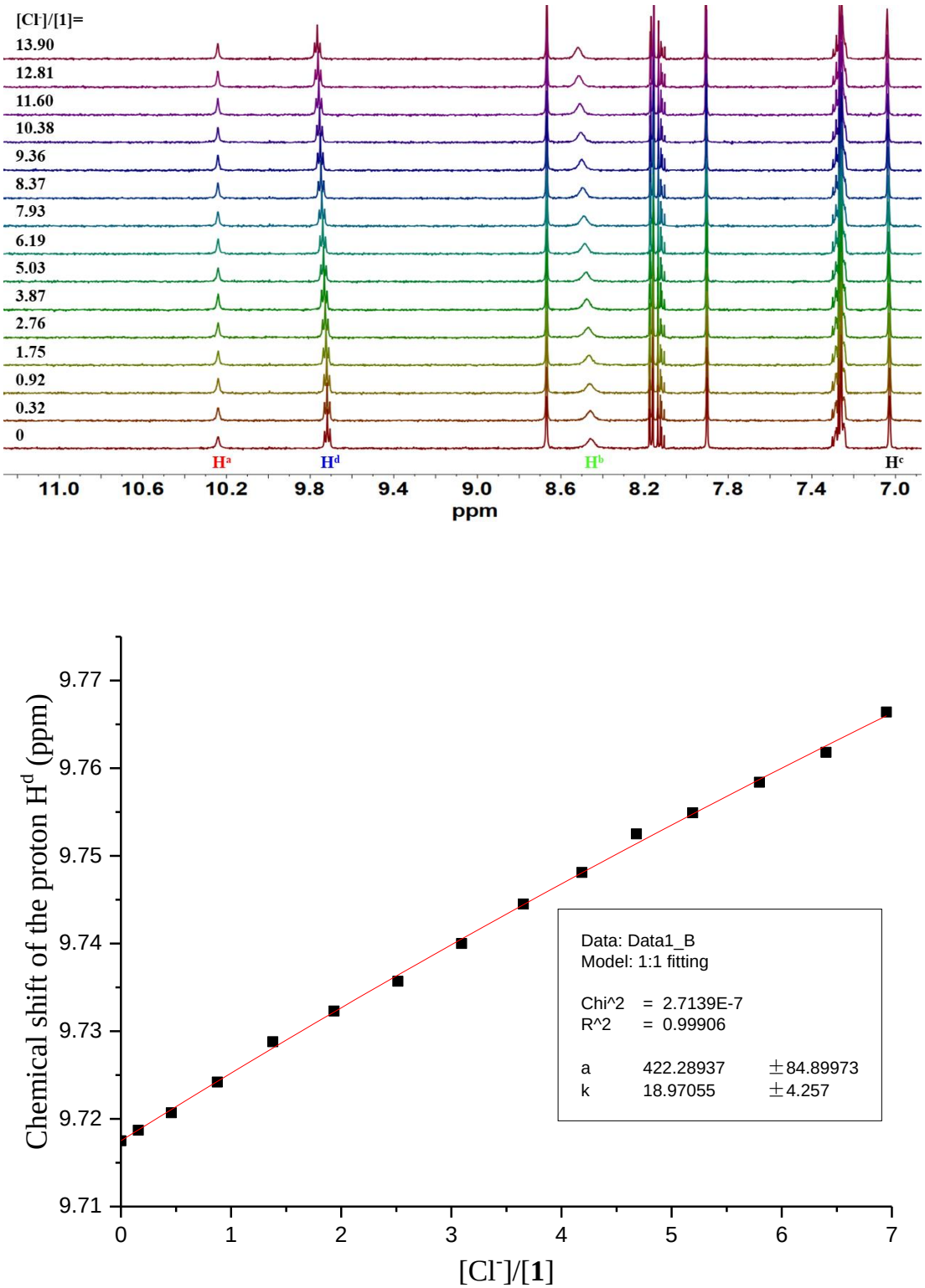

Fig. S5 Top: Stack plot of ^{1}H NMR titration of macrocycle **1** (1.0 mM) with ^{n}Bu$_4$NCl in DMSO-d_6 at 298 K. Bottom: The non-linear curve fitting of the chemical shifts for amide NH signals (H^{d}) in macrocycle **1** against equivalents of Cl^{-}, assuming a 1:1 binding model.

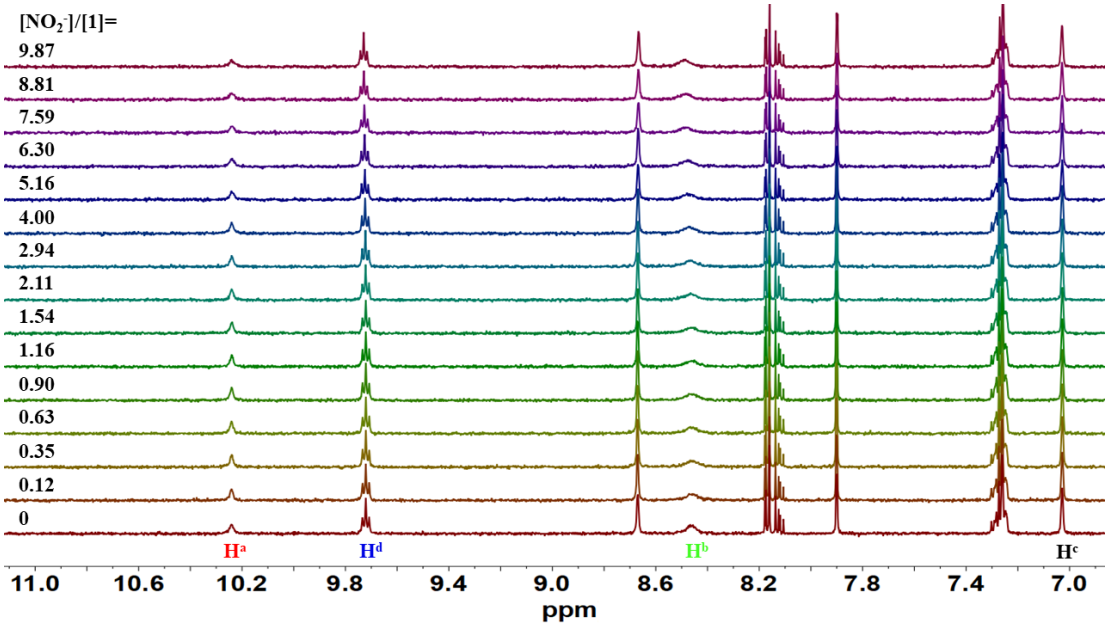

Fig. S6 Stack plot of ^{1}H NMR titration of macrocycle **1** (1.0 mM) with $^{n}Bu_4NNO_2$ in DMSO-d_6 at 298 K.

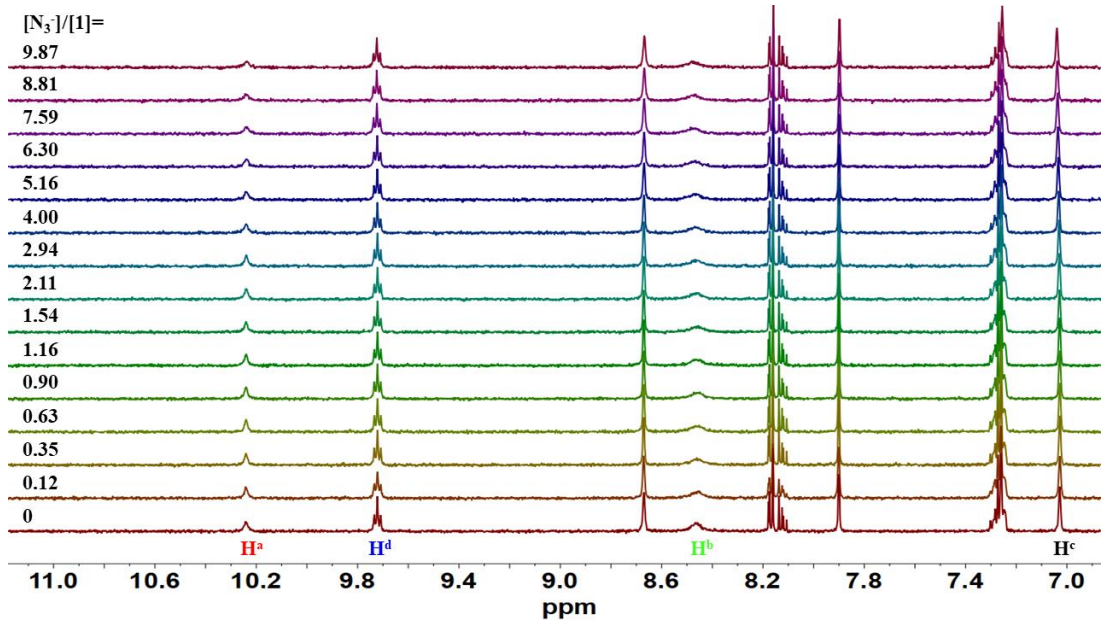

Fig. S7 Stack plot of ^{1}H NMR titration of macrocycle **1** (1.0 mM) with $^{n}Bu_4NN_3$ in DMSO-d_6 at 298 K.

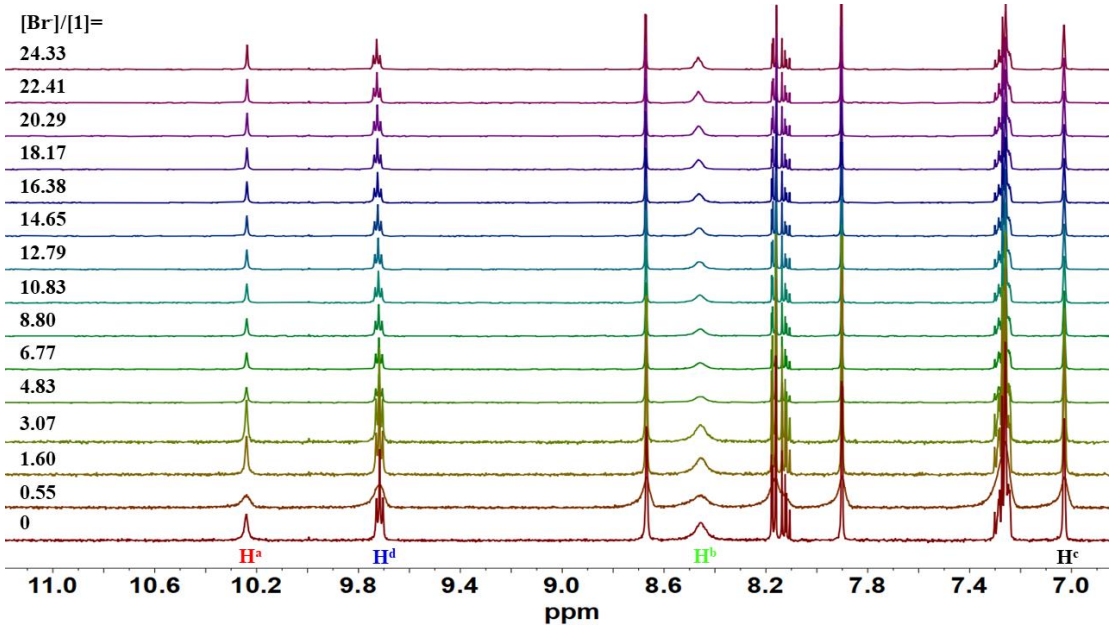

Fig. S8 Stack plot of ^{1}H NMR titration of macrocycle **1** (1.0 mM) with ^{n}Bu$_4$NBr in DMSO-d_6 at 298 K.

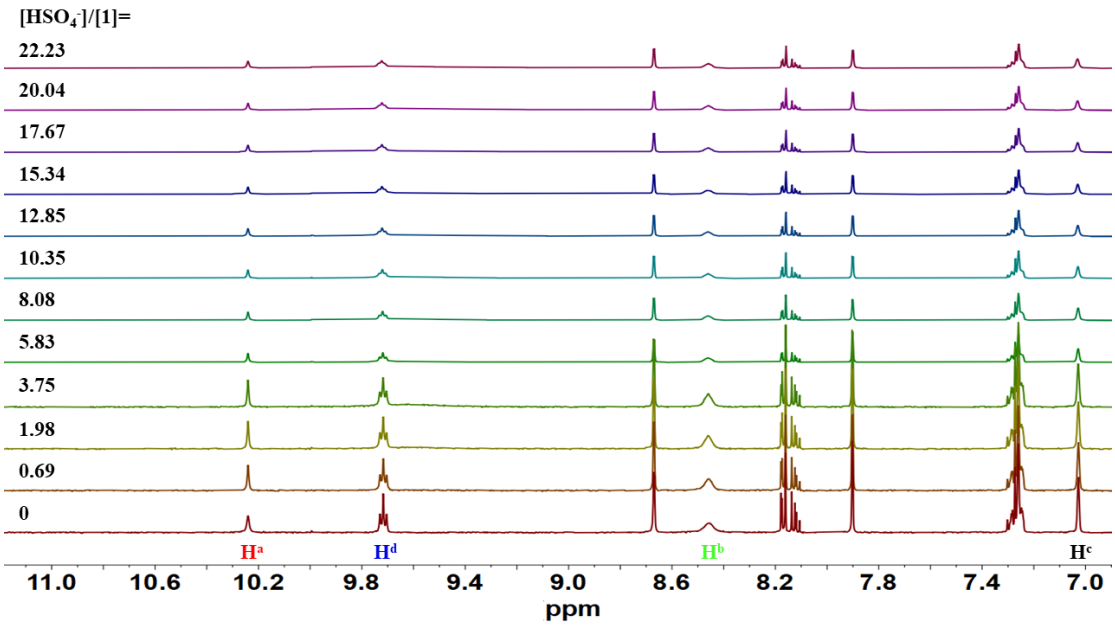

Fig. S9 Stack plot of ^{1}H NMR titration of macrocycle **1** (1.0 mM) with ^{n}Bu$_4$NHSO$_4$ in DMSO-d_6 at 298 K.

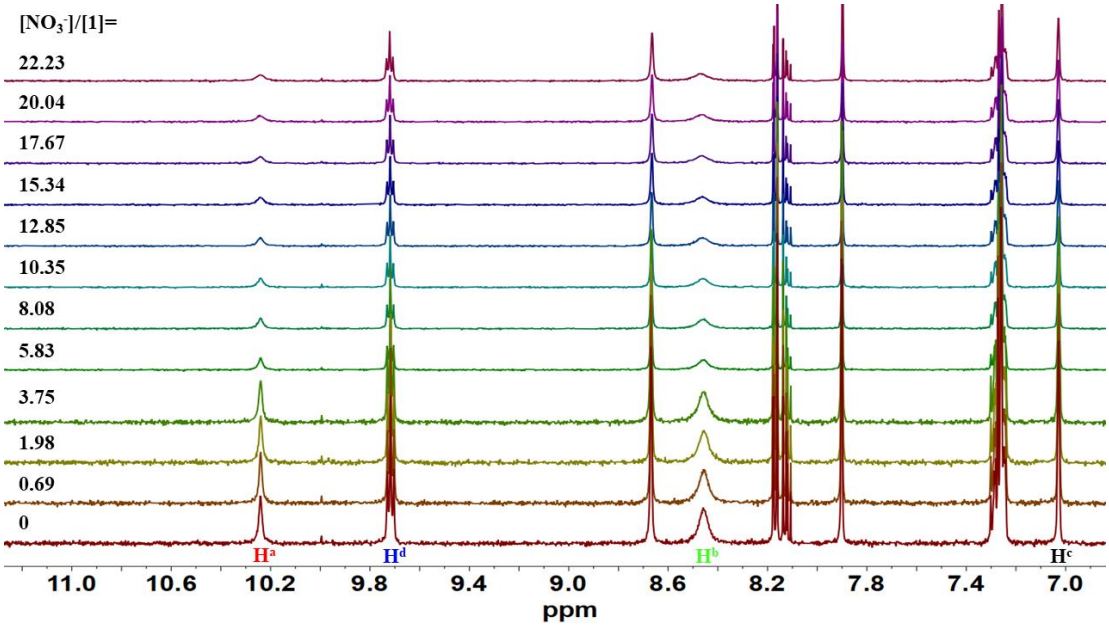

Fig. S10 Stack plot of ^{1}H NMR titration of macrocycle **1** (1.0 mM) with $^{n}Bu_4NNO_3$ in DMSO-d_6 at 298 K.

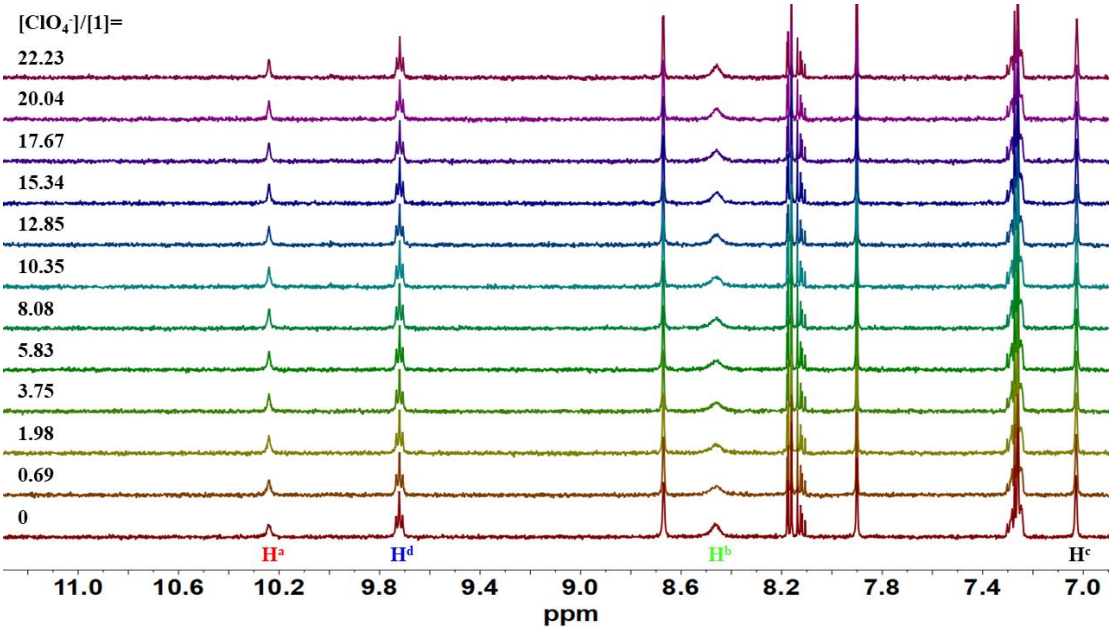

Fig. S11 Stack plot of ^{1}H NMR titration of macrocycle **1** (1.0 mM) with $^{n}Bu_4NClO_4$ in DMSO-d_6 at 298 K.

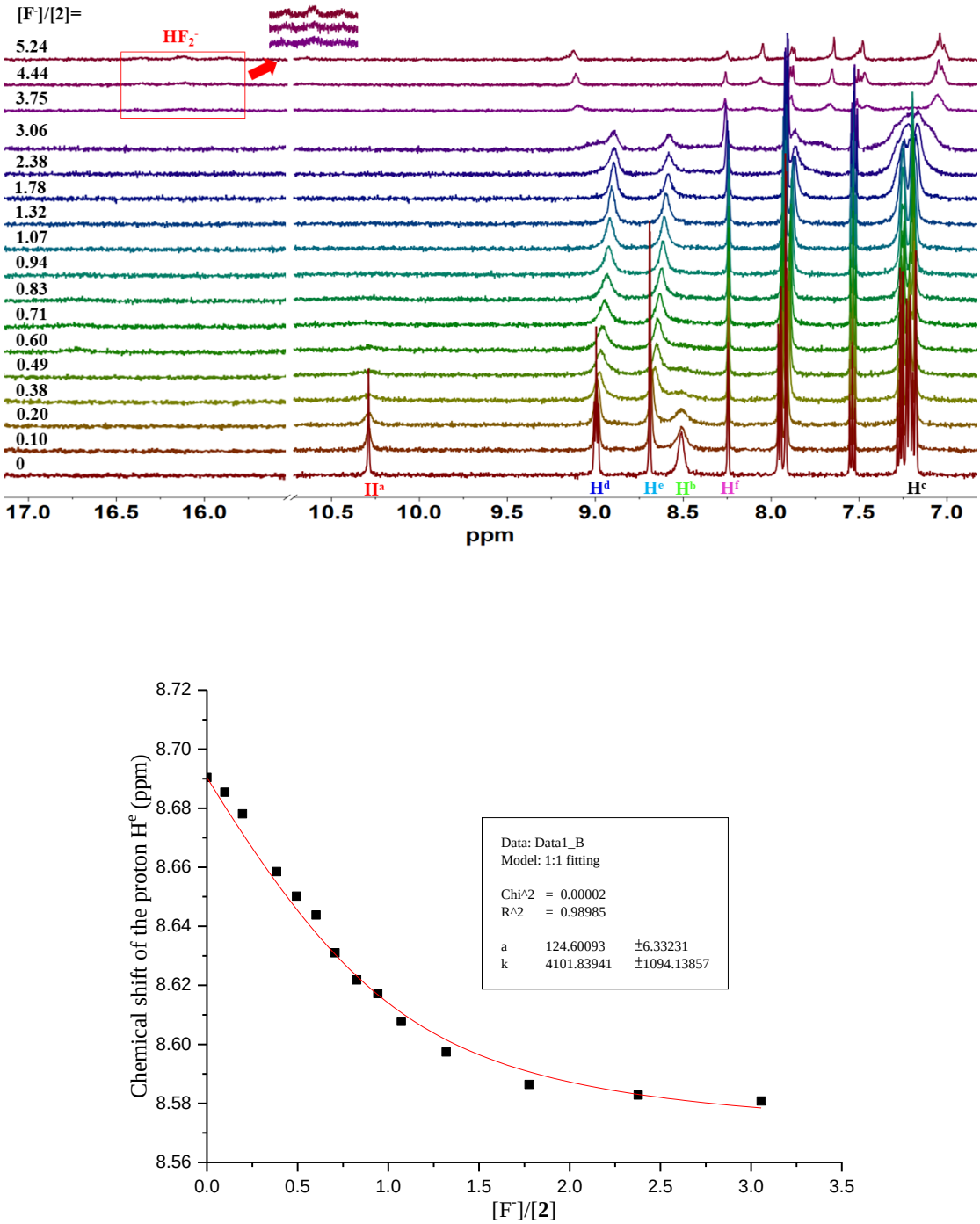

Fig. S12 Top: Stack plot of ^{1}H NMR titration of macrocycle **2** (1.0 mM) with ^{n}Bu$_4$NF in DMSO-d_6 at 298 K. Bottom: The non-linear curve fitting of the chemical shifts for carbazole CH signals (H^e) in macrocycle **2** against equivalents of F^-, assuming a 1:1 binding model.

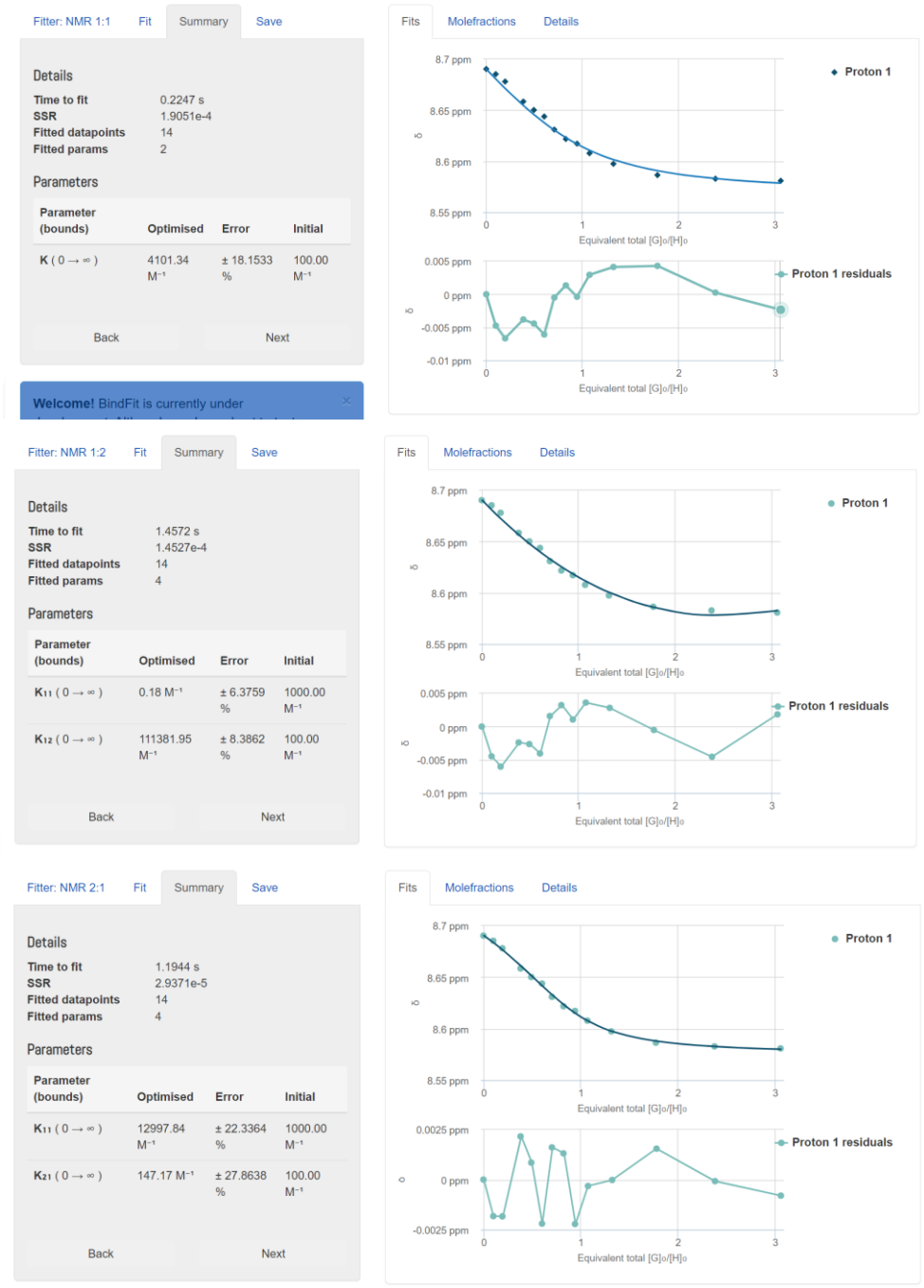

Fig. S13 Top: The corresponding isotherm of macrocycle **2** with ^{n}Bu$_4$NF based on a 1:1 model using the www.supramolecular.org web applet, giving $K_a = 4101$ M^{-1}. The monitored signal was carbazole CH (H^e) protons. The residual distribution was displayed below the binding isotherm. Middle: The corresponding isotherm of macrocycle **2** with ^{n}Bu$_4$NF based on a 1:2 model using the www.supramolecular.org web applet, giving $K_{11} = 0.18$ M^{-1} and $K_{12} = 111382$ M^{-1}. The monitored signal was carbazole CH (H^e) protons. The residual distribution was displayed below the binding isotherm. Bottom: The corresponding isotherm of macrocycle **2** with ^{n}Bu$_4$NF based on a 2:1 model using the www.supramolecular.org web applet, giving $K_{11} = 12998$ M^{-1} and $K_{21} = 147$ M^{-1}. The monitored signal was carbazole CH (H^e) protons. The residual distribution was displayed below the binding isotherm. Considering the errors and reasonability in the calculation of binding constants using the 1:2 and 2:1 models, the use of a 1:1 model was the most reliable.

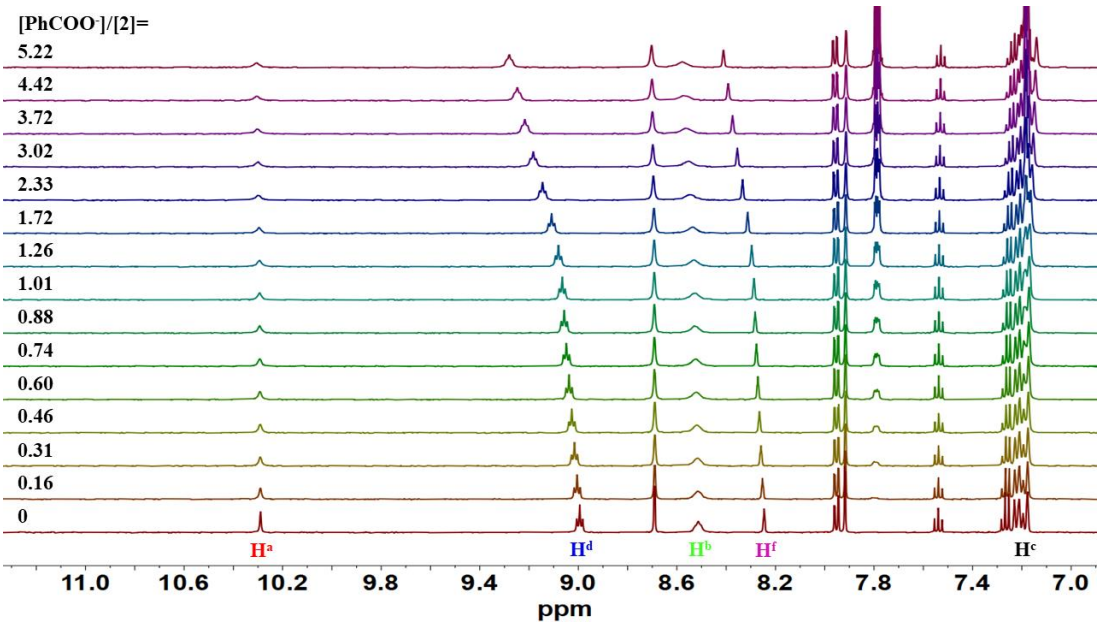

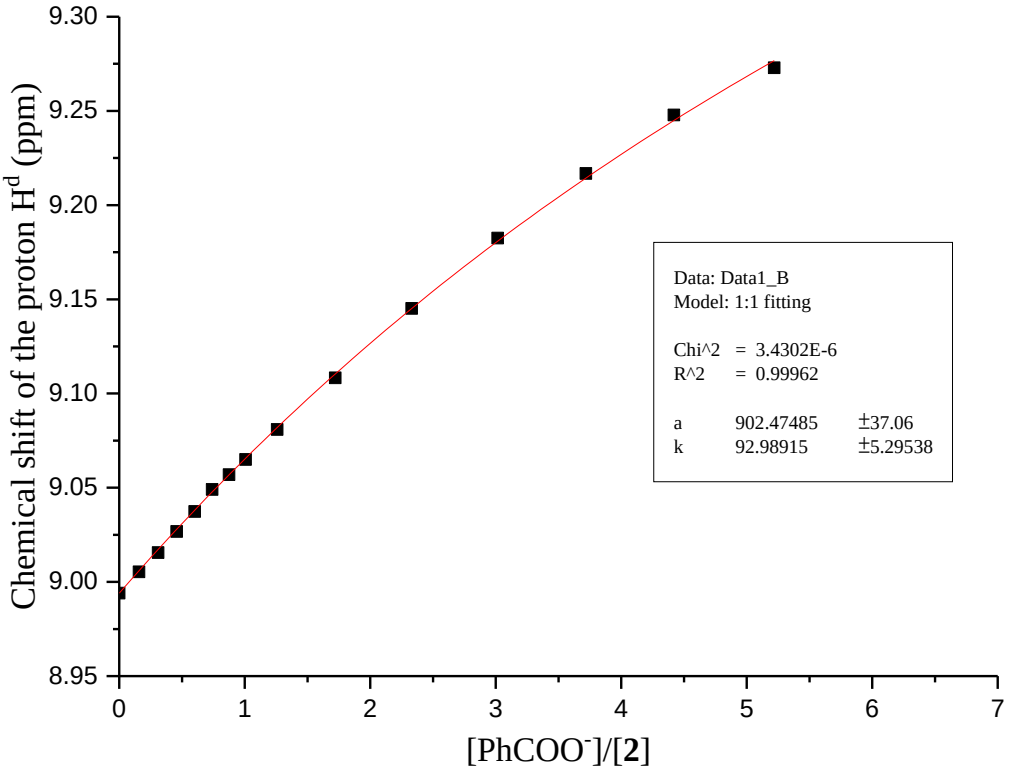

Fig. S14 Top: Stack plot of ^{1}H NMR titration of macrocycle **2** (1.0 mM) with ^{n}Bu$_4$NPhCOO in DMSO-d_6 at 298 K. Bottom: The non-linear curve fitting of the chemical shifts for amide NH signals (H^d) in macrocycle **2** against equivalents of PhCOO$^-$, assuming a 1:1 binding model.

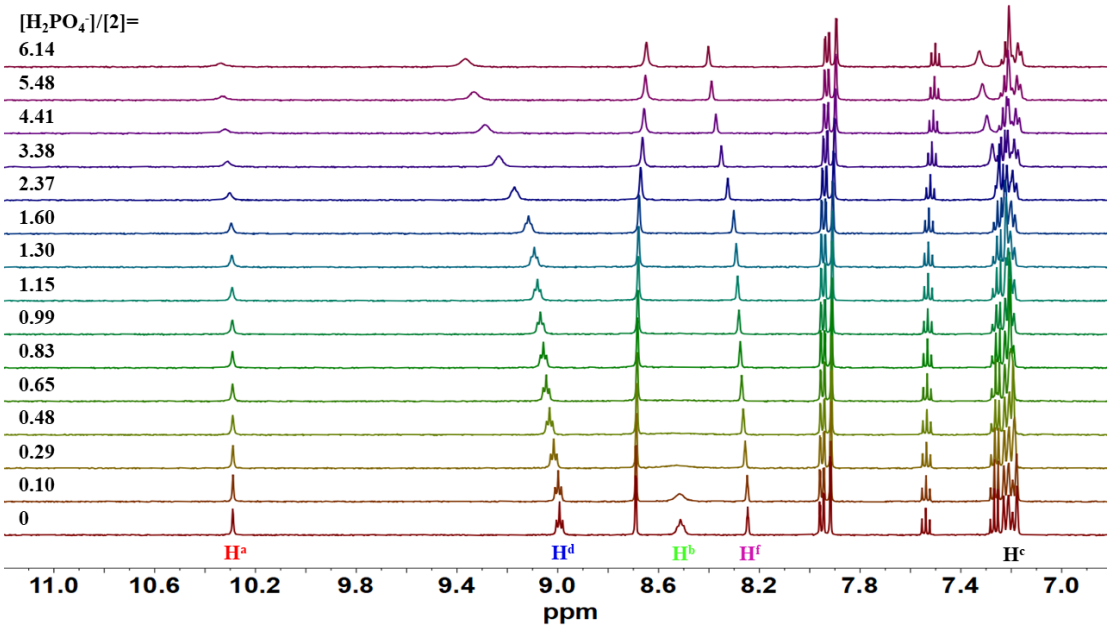

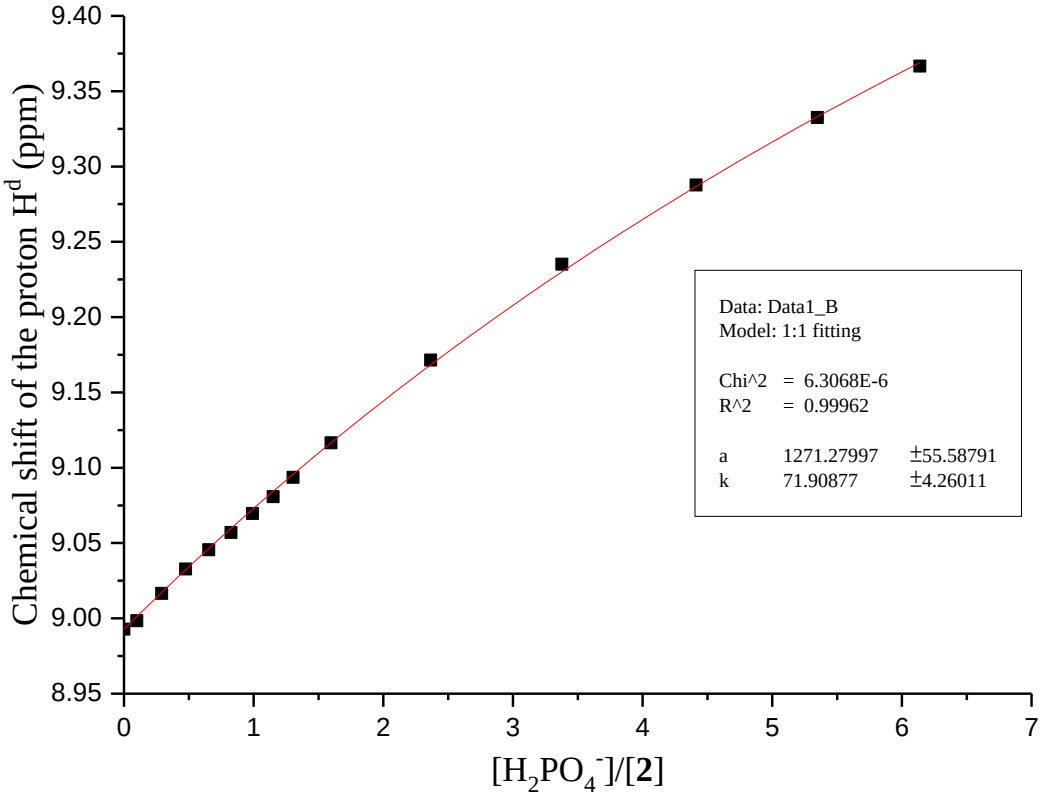

Fig. S15 Top: Stack plot of ^{1}H NMR titration of macrocycle **2** (1.0 mM) with $^{n}Bu_4NH_2PO_4$ in DMSO-d_6 at 298 K. Bottom: The non-linear curve fitting of the chemical shifts for amide NH signals (H^d) in macrocycle **2** against equivalents of $H_2PO_4^-$, assuming a 1:1 binding model.

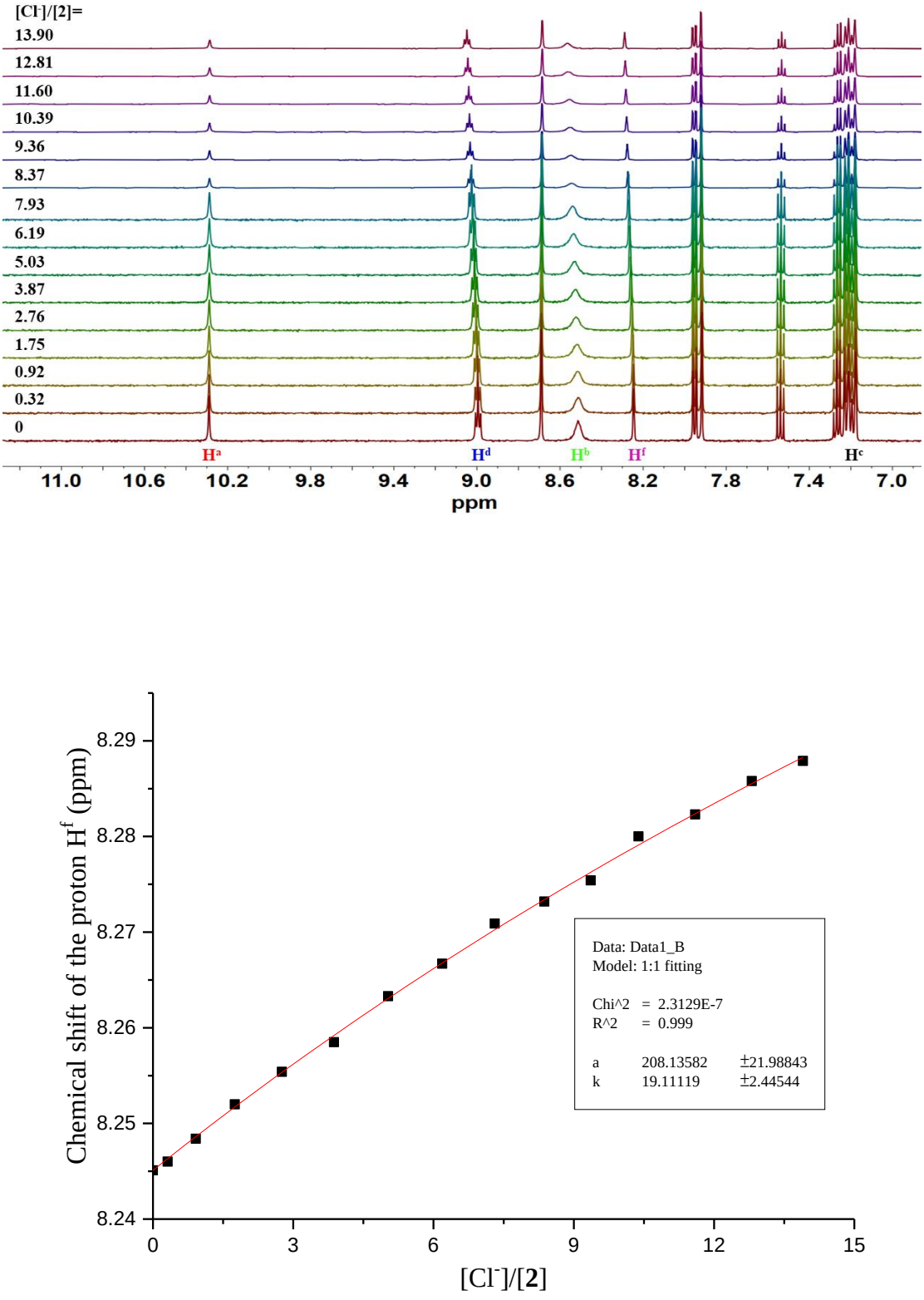

Fig. S16 Top: Stack plot of ^{1}H NMR titration of macrocycle **2** (1.0 mM) with ^{n}Bu$_4$NCl in DMSO-d_6 at 298 K. Bottom: The non-linear curve fitting of the chemical shift for aromatic CH signal (H^f) in macrocycle **2** against equivalents of Cl^-, assuming a 1:1 binding model.

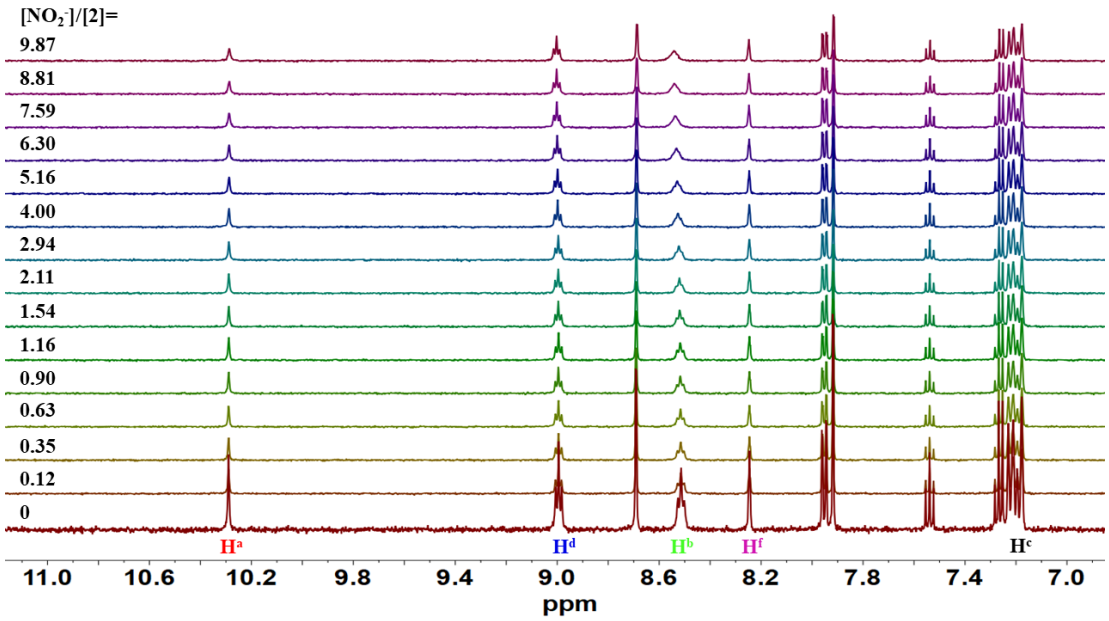

Fig. S17 Stack plot of ^{1}H NMR titration of macrocycle **2** (1.0 mM) with $^{n}Bu_4NNO_2$ in DMSO-d_6 at 298 K.

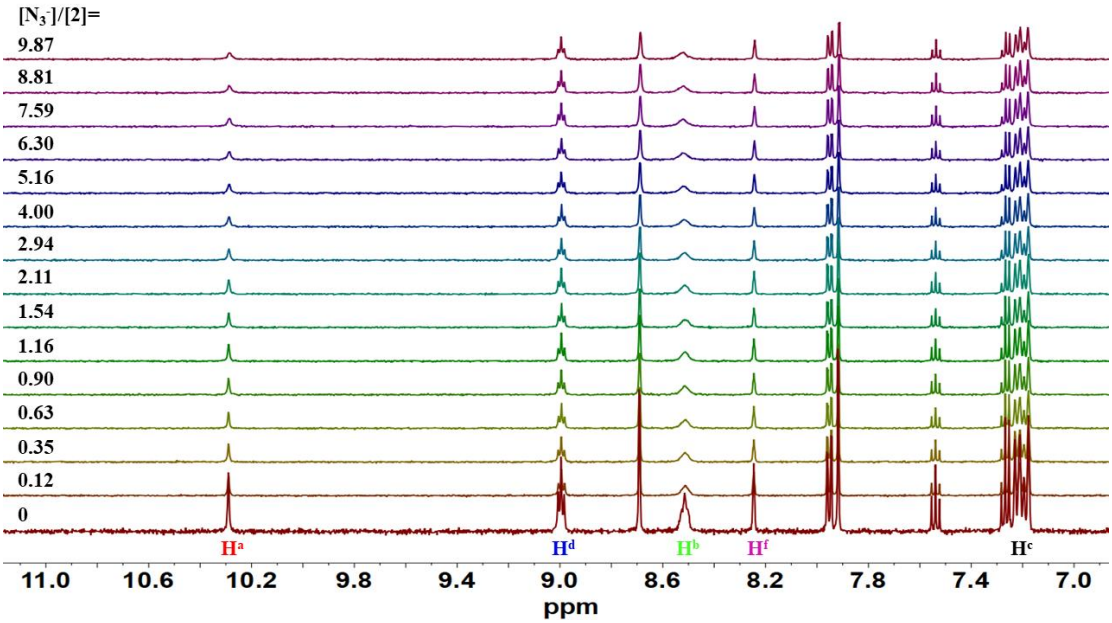

Fig. S18 Stack plot of ^{1}H NMR titration of macrocycle **2** (1.0 mM) with $^{n}Bu_4NN_3$ in DMSO-d_6 at 298 K.

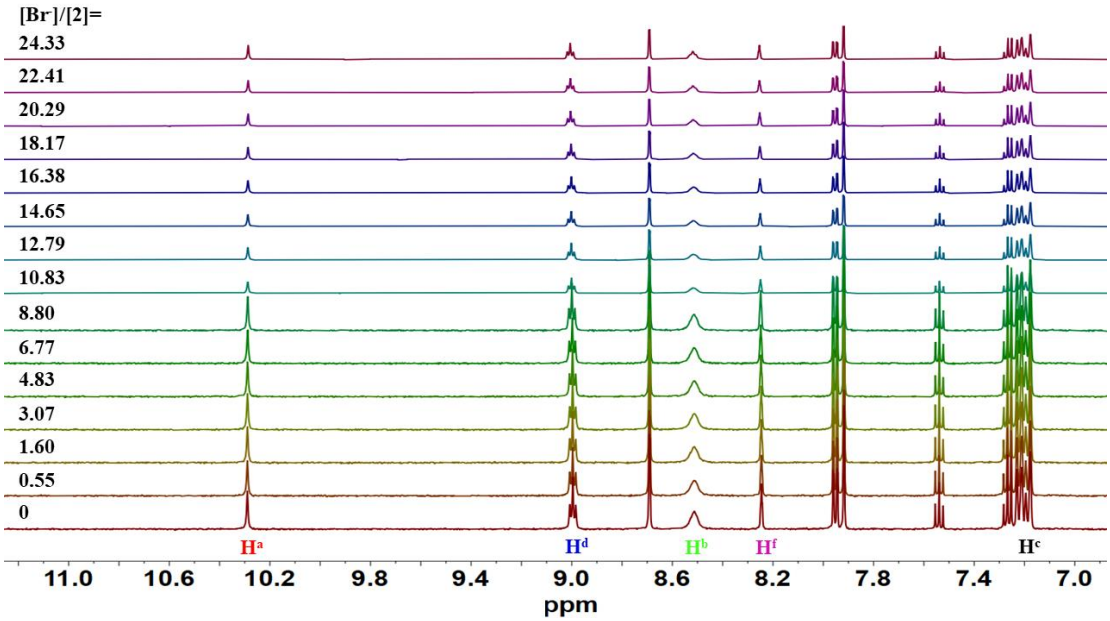

Fig. S19 Stack plot of ^{1}H NMR titration of macrocycle **2** (1.0 mM) with ^{n}Bu$_4$NBr in DMSO-d_6 at 298 K.

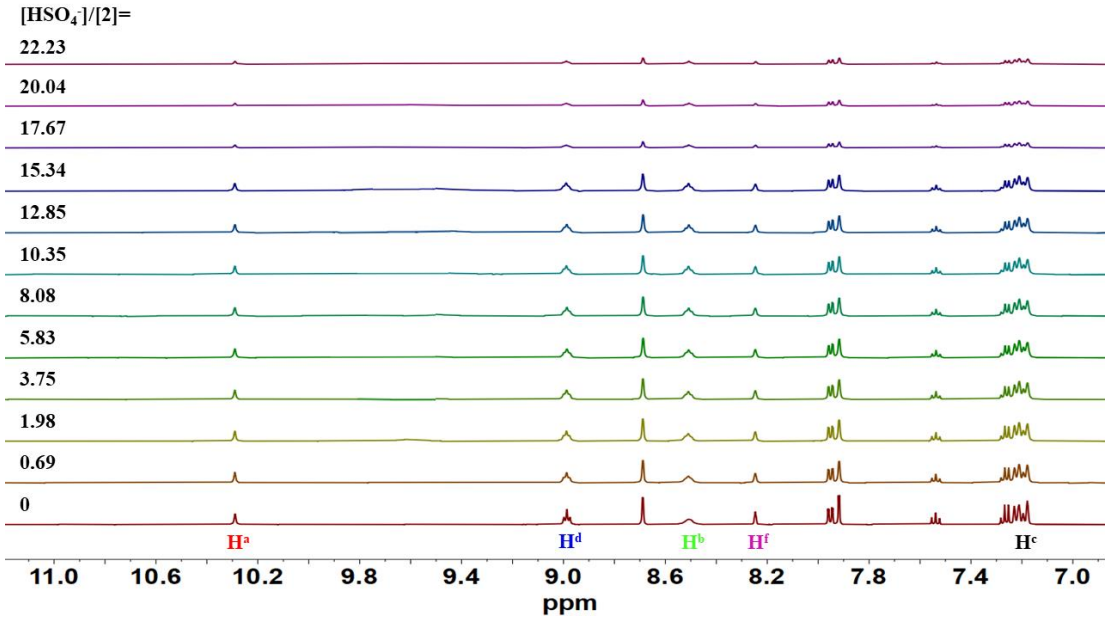

Fig. S20 Stack plot of ^{1}H NMR titration of macrocycle **2** (1.0 mM) with ^{n}Bu$_4$NHSO$_4$ in DMSO-d_6 at 298 K.

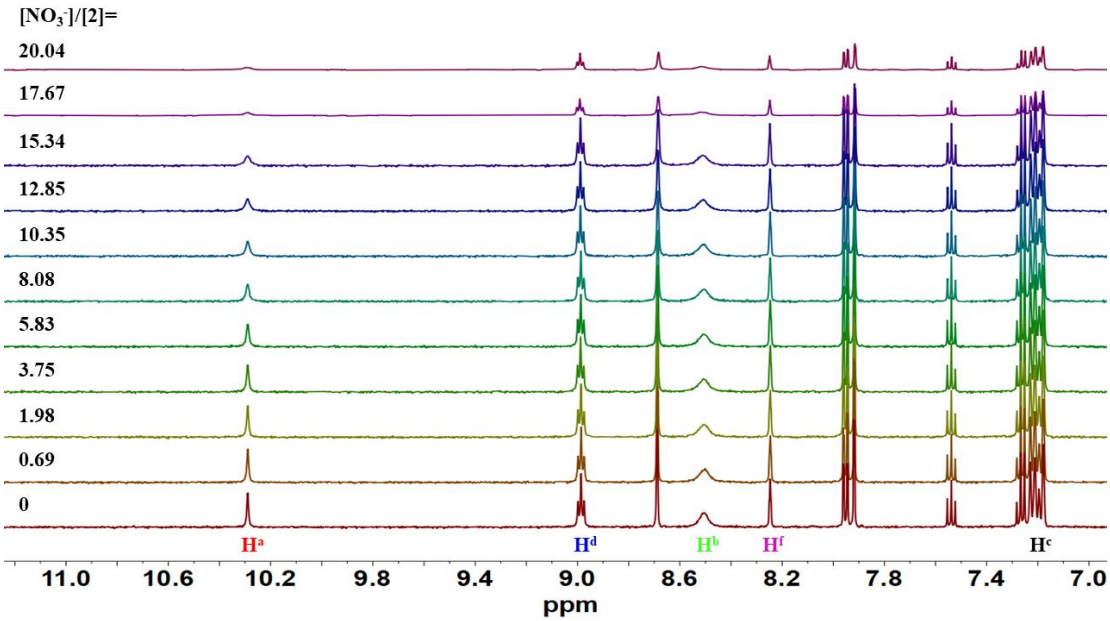

Fig. S21 Stack plot of ^{1}H NMR titration of macrocycle **2** (1.0 mM) with $^{n}Bu_4NNO_3$ in DMSO-d_6 at 298 K.

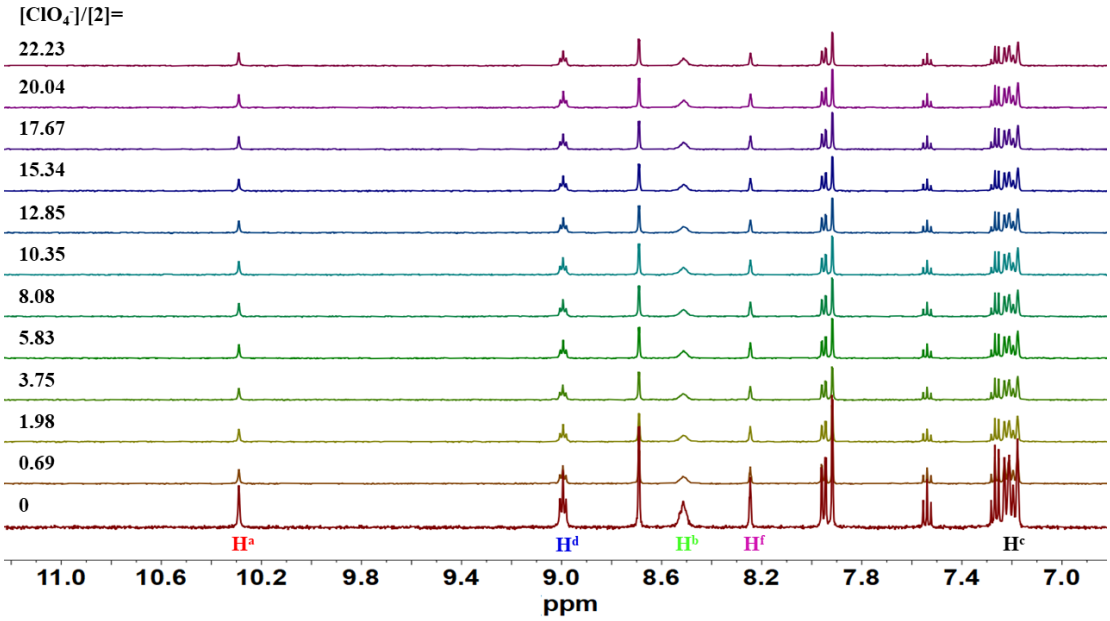

Fig. S22 Stack plot of ^{1}H NMR titration of macrocycle **2** (1.0 mM) with $^{n}Bu_4NClO_4$ in DMSO-d_6 at 298 K.

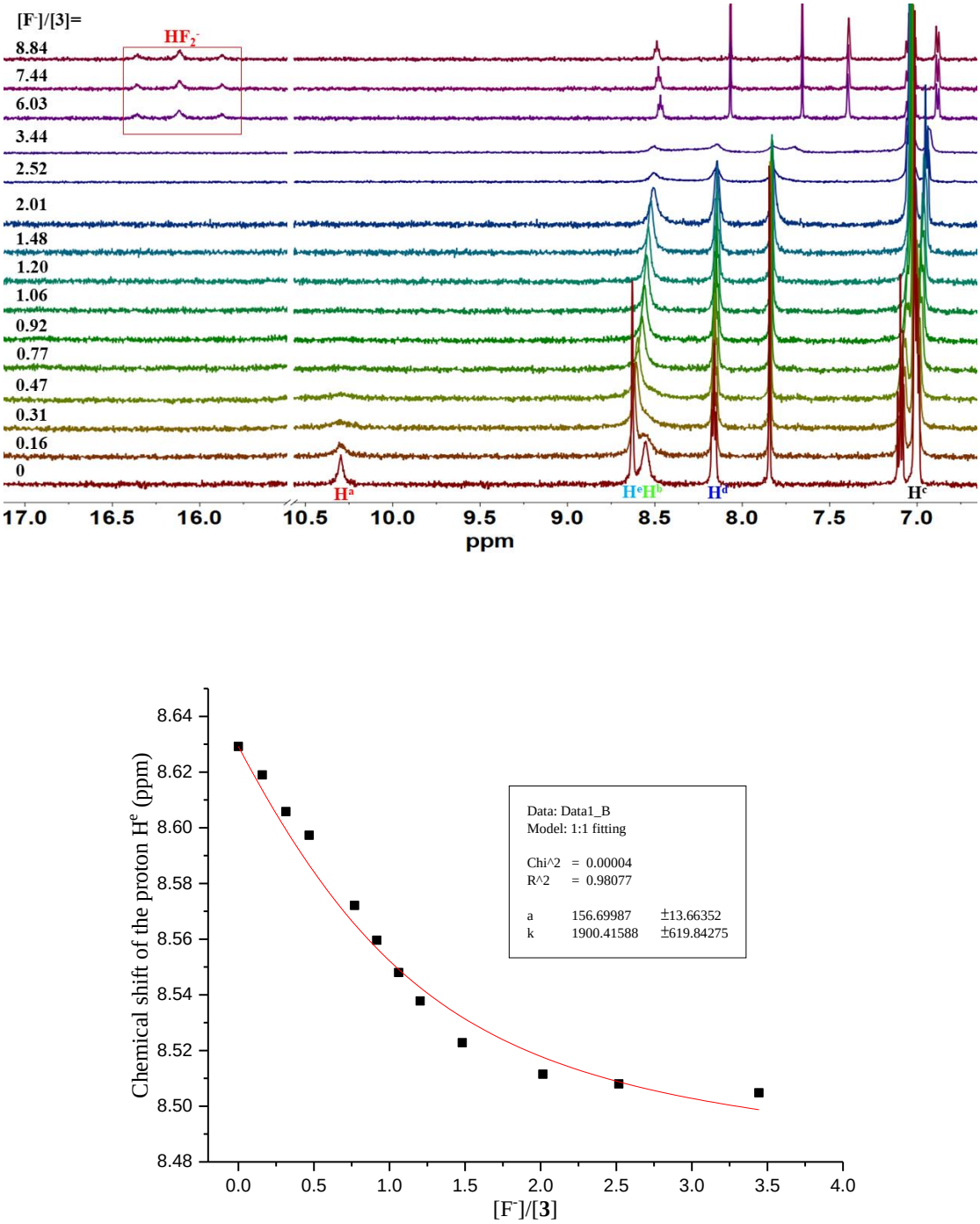

Fig. S23 Top: Stack plot of ^{1}H NMR titration of acyclic receptor **3** (1.0 mM) with ^{n}Bu$_4$NF in DMSO-d_6 at 298 K. Bottom: The non-linear curve fitting of the chemical shifts for carbazole CH signals (H^e) in acyclic receptor **3** against equivalents of F^-, assuming a 1:1 binding model.

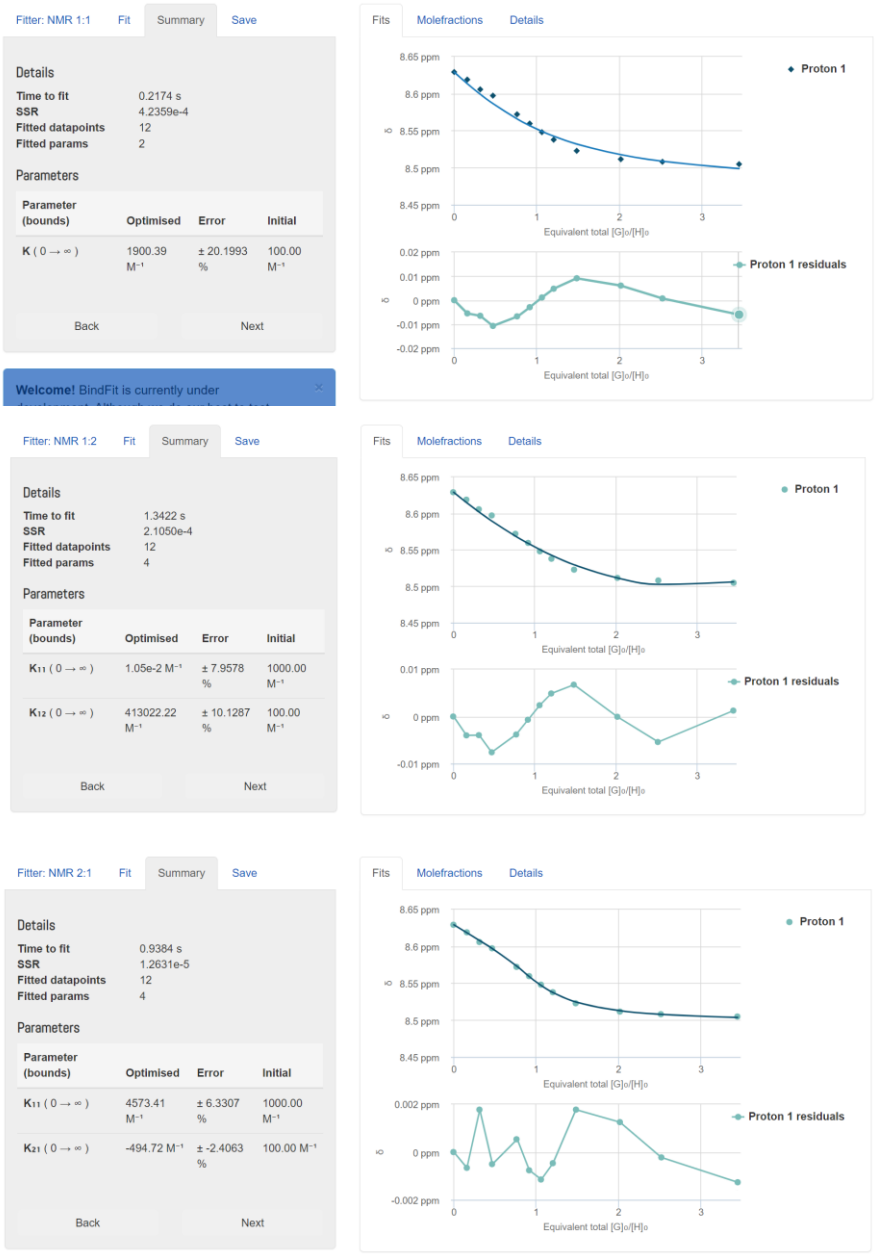

Fig. S24 Top: The corresponding isotherm of acyclic receptor **3** with ^{n}Bu$_4$NF based on a 1:1 model using the www.supramolecular.org web applet, giving K_a = 1900 M^{-1}. The monitored signal was carbazole CH (H^e) protons. The residual distribution was displayed below the binding isotherm. Middle: The corresponding isotherm of acyclic receptor **3** with ^{n}Bu$_4$NF based on a 1:2 model using the www.supramolecular.org web applet, giving K_{11} = 0.01 M^{-1} and K_{12} = 413022 M^{-1}. The monitored signal was carbazole CH (H^e) protons. The residual distribution was displayed below the binding isotherm. Bottom: The corresponding isotherm of acyclic receptor **3** with ^{n}Bu$_4$NF based on a 2:1 model using the www.supramolecular.org web applet, giving K_{11} = 4573 M^{-1} and K_{21} = –495 M^{-1}. The monitored signal was carbazole CH (H^e) protons. The residual distribution was displayed below the binding isotherm. Considering the errors and negative values in the calculation of binding constants using the 1:2 and 2:1 models, the use of a 1:1 model was the most reasonable and reliable.

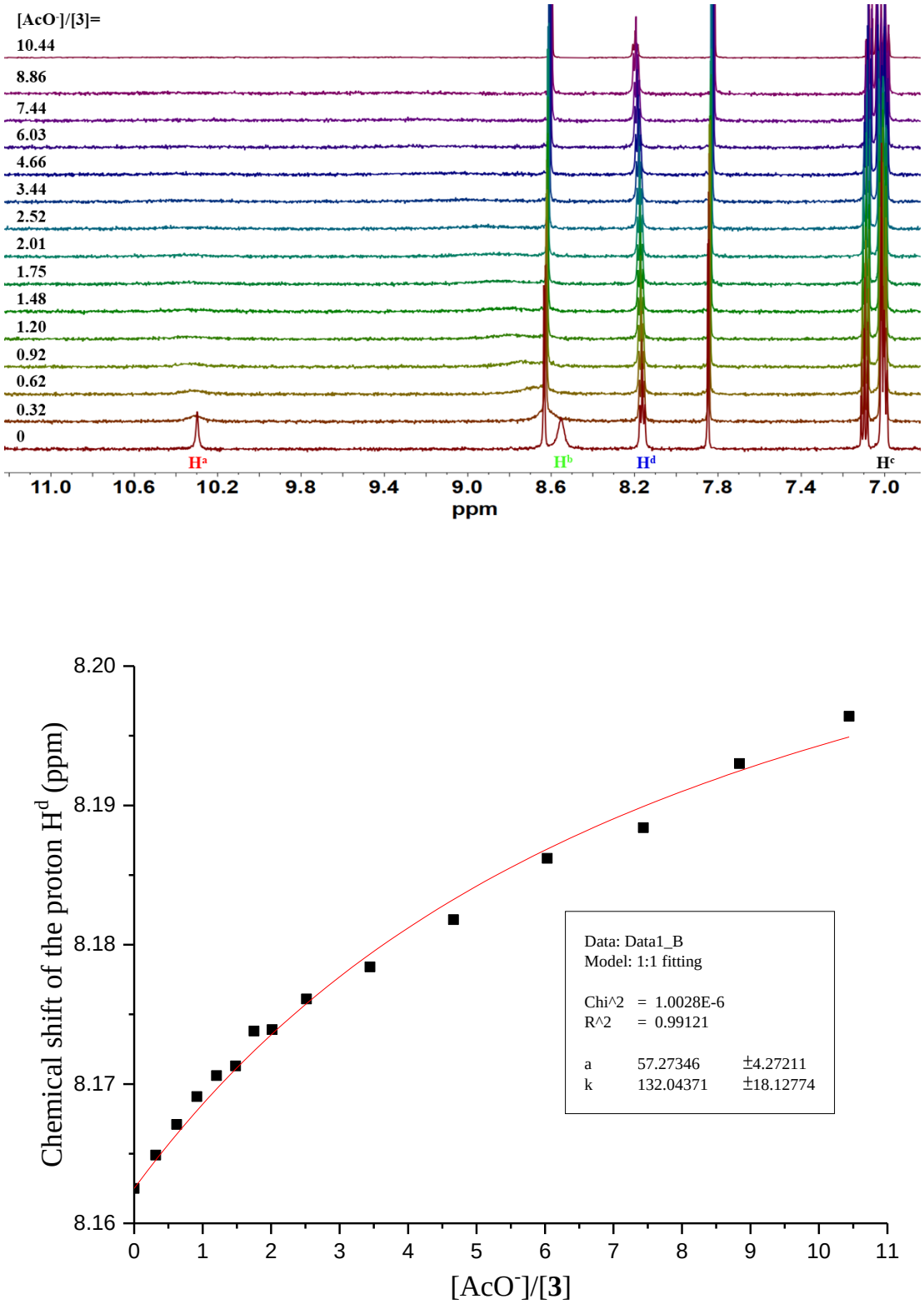

Fig. S25 Top: Stack plot of ^{1}H NMR titration of acyclic receptor **3** (1.0 mM) with ^{n}Bu$_4$NAcO in DMSO-d_6 at 298 K. Bottom: The non-linear curve fitting of the chemical shifts for amide NH signals (H^d) in acyclic receptor **3** against equivalents of AcO$^-$, assuming a 1:1 binding model.

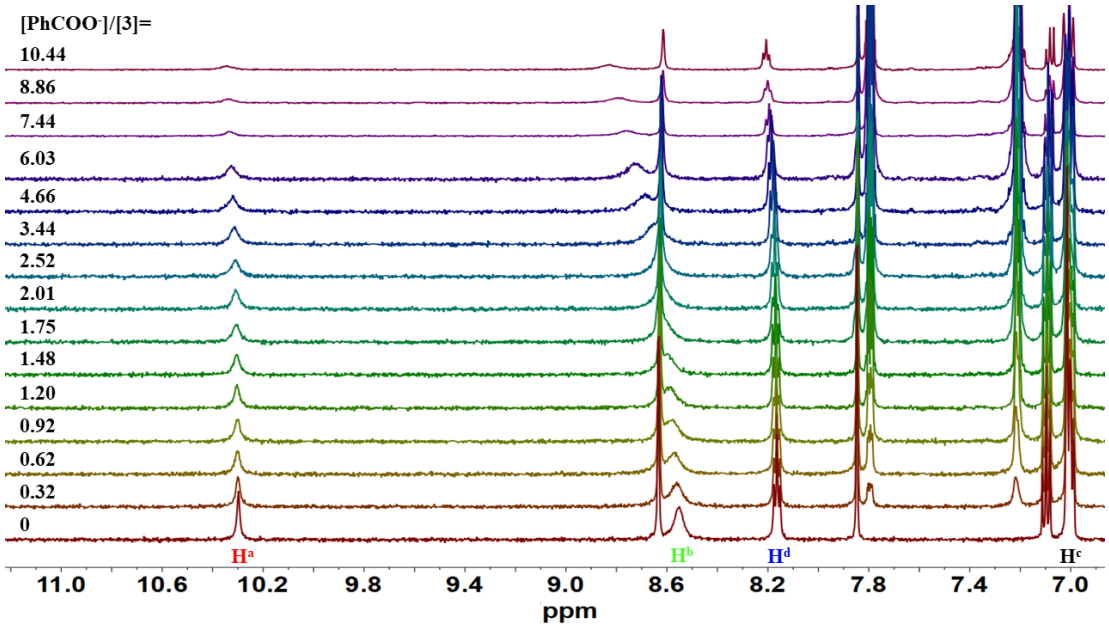

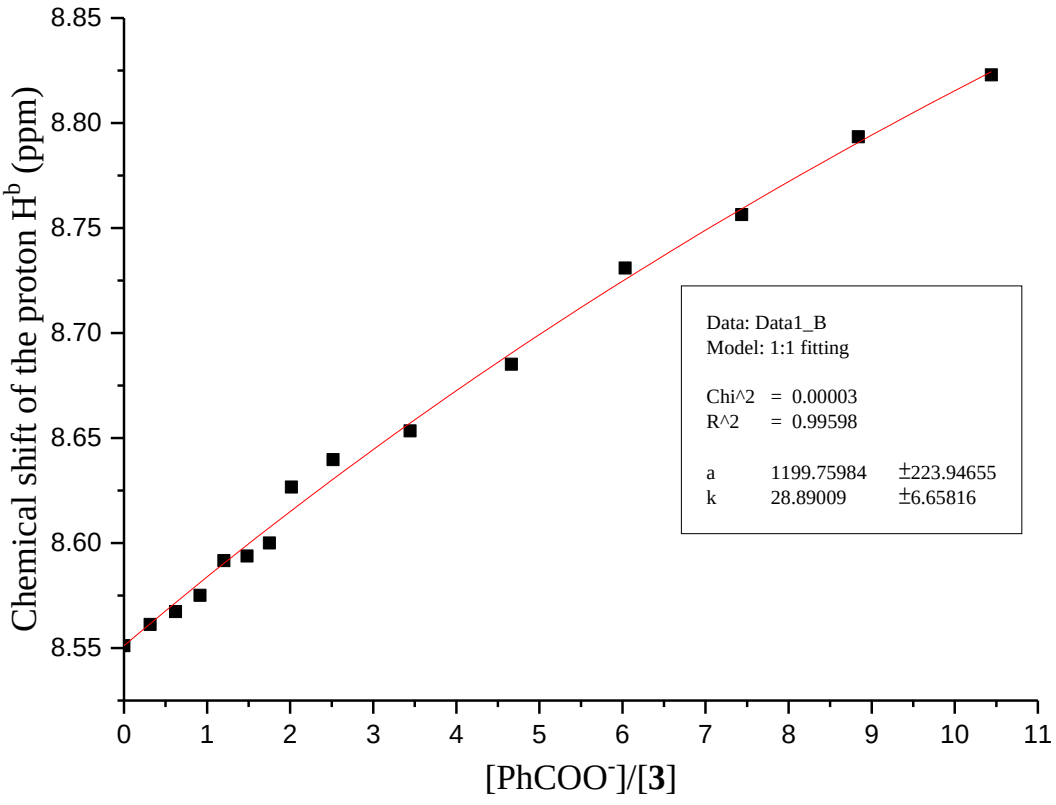

Fig. S26 Top: Stack plot of ^{1}H NMR titration of acyclic receptor **3** (1.0 mM) with ^{n}Bu$_4$NPhCOO in DMSO-d_6 at 298 K. Bottom: The non-linear curve fitting of the chemical shifts for sulfonamide NH signals (H^b) in acyclic receptor **3** against equivalents of PhCOO$^-$, assuming a 1:1 binding model.

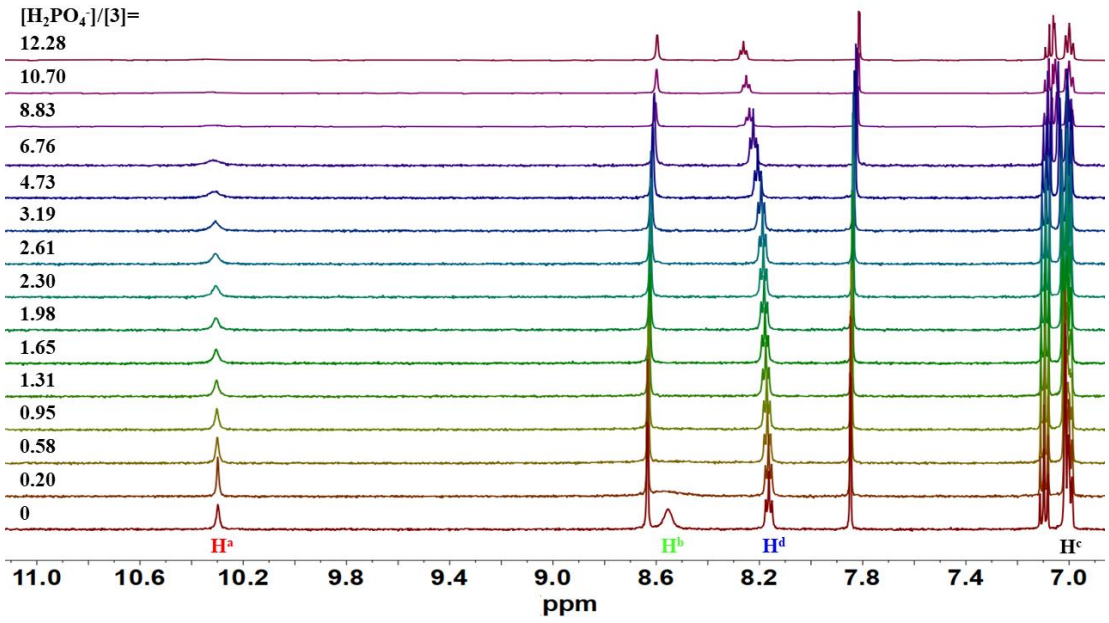

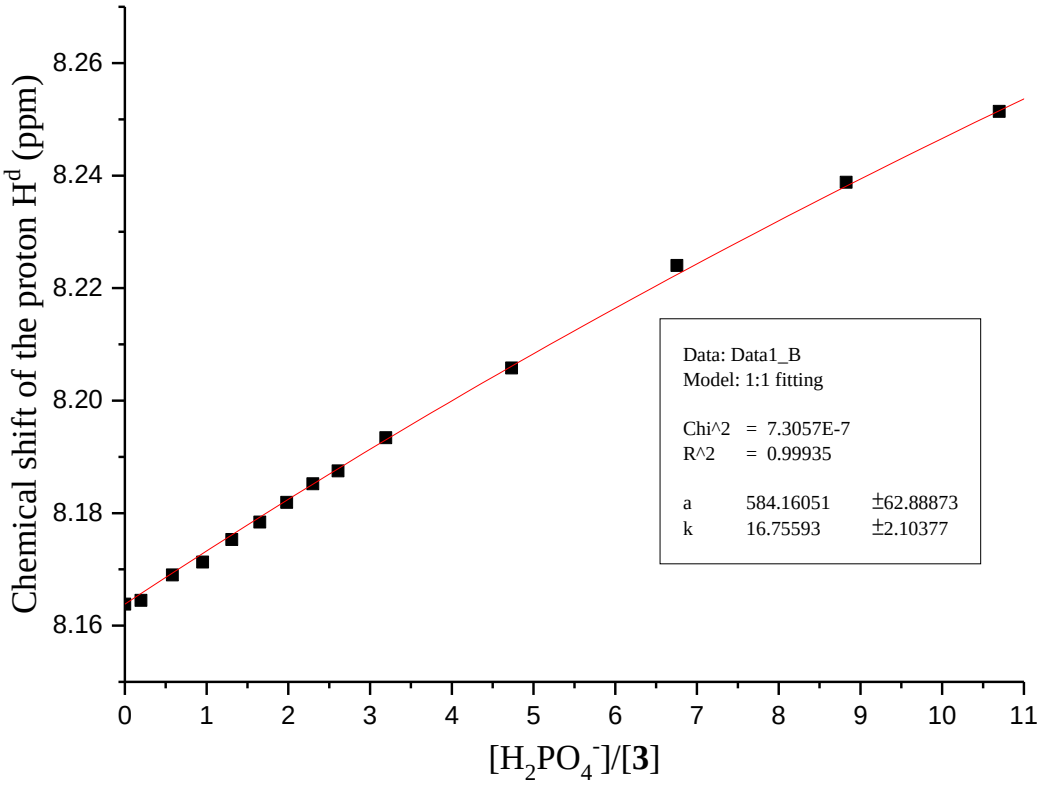

Fig. S27 Top: Stack plot of ^{1}H NMR titration of acyclic receptor **3** (1.0 mM) with $^{n}Bu_4NH_2PO_4$ in DMSO-d_6 at 298 K. Bottom: The non-linear curve fitting of the chemical shifts for amide NH signals (H^d) in acyclic receptor **3** against equivalents of $H_2PO_4^-$, assuming a 1:1 binding model.

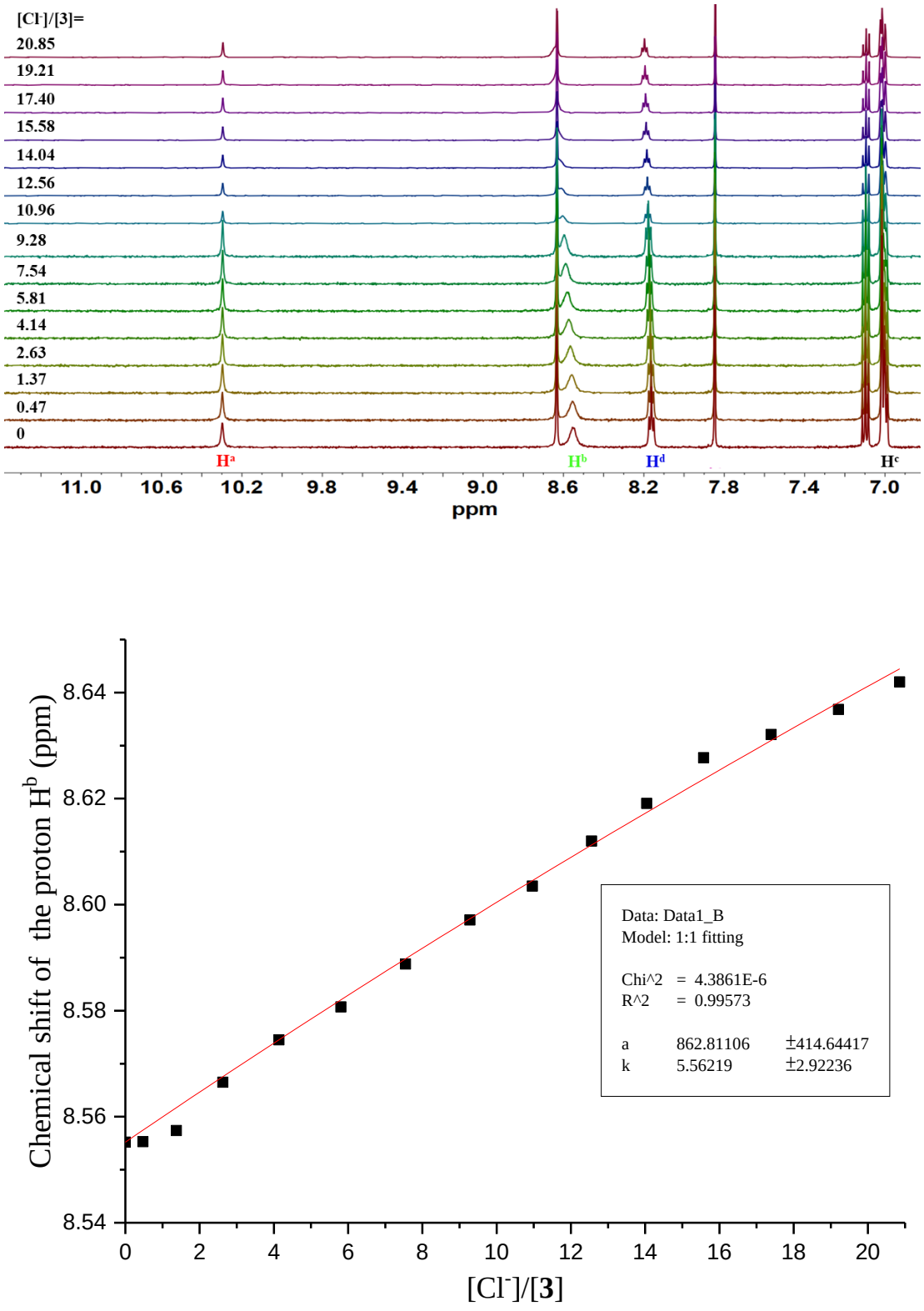

Fig. S28 Top: Stack plot of ^{1}H NMR titration of acyclic receptor **3** (1.0 mM) with ^{n}Bu$_4$NCl in DMSO-d_6 at 298 K. Bottom: The non-linear curve fitting of the chemical shifts for sulfonamide NH signals (H^b) in acyclic receptor **3** against equivalents of Cl$^-$, assuming a 1:1 binding model.

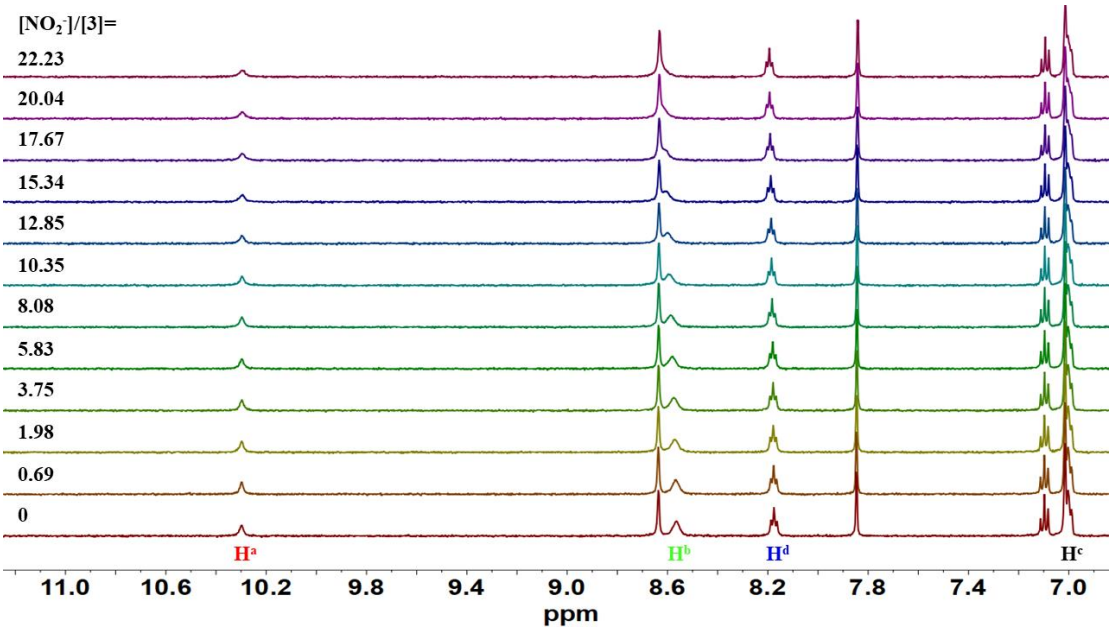

Fig. S29 Stack plot of ^{1}H NMR titration of acyclic receptor **3** (1.0 mM) with $^{n}Bu_4NNO_2$ in DMSO-d_6 at 298 K.

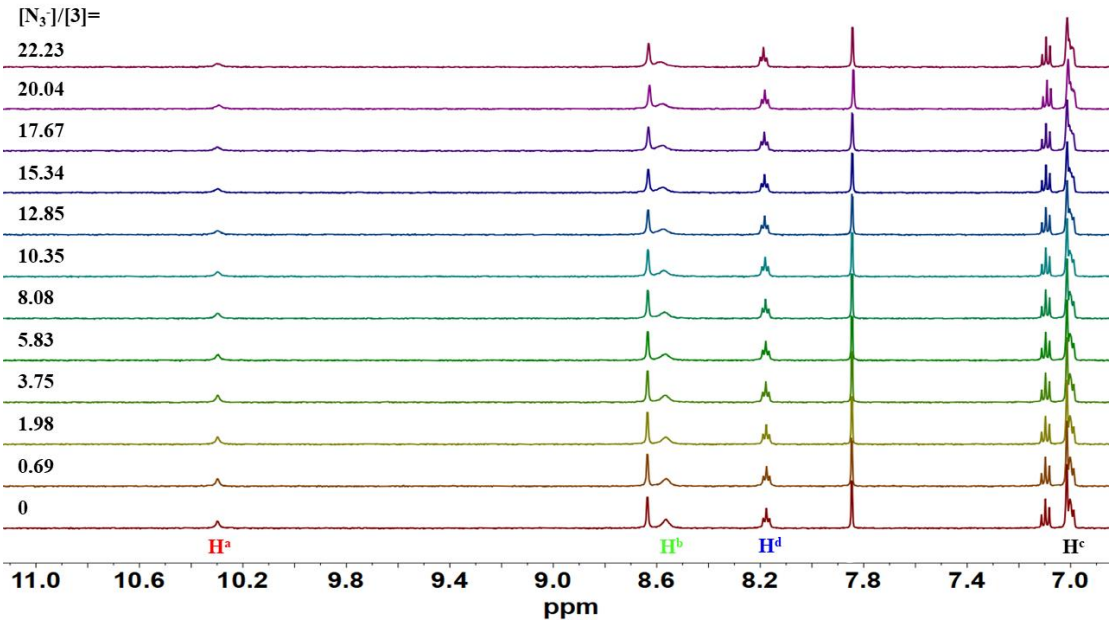

Fig. S30 Stack plot of ^{1}H NMR titration of acyclic receptor **3** (1.0 mM) with $^{n}Bu_4NN_3$ in DMSO-d_6 at 298 K.

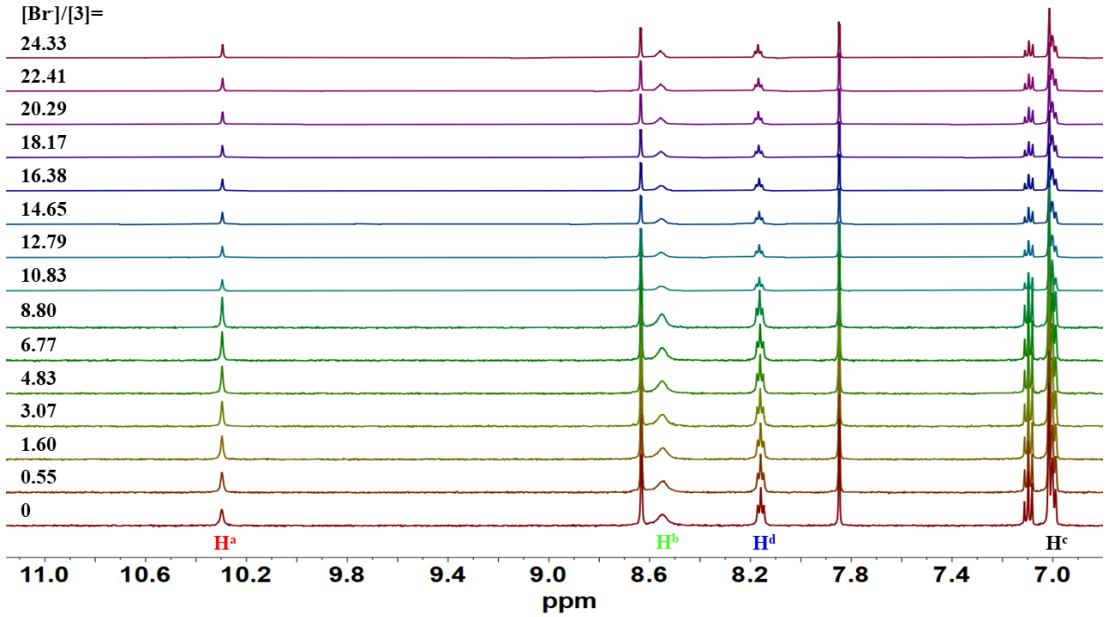

Fig. S31 Stack plot of ^{1}H NMR titration of acyclic receptor **3** (1.0 mM) with ^{n}Bu$_4$NBr in DMSO-d_6 at 298 K.

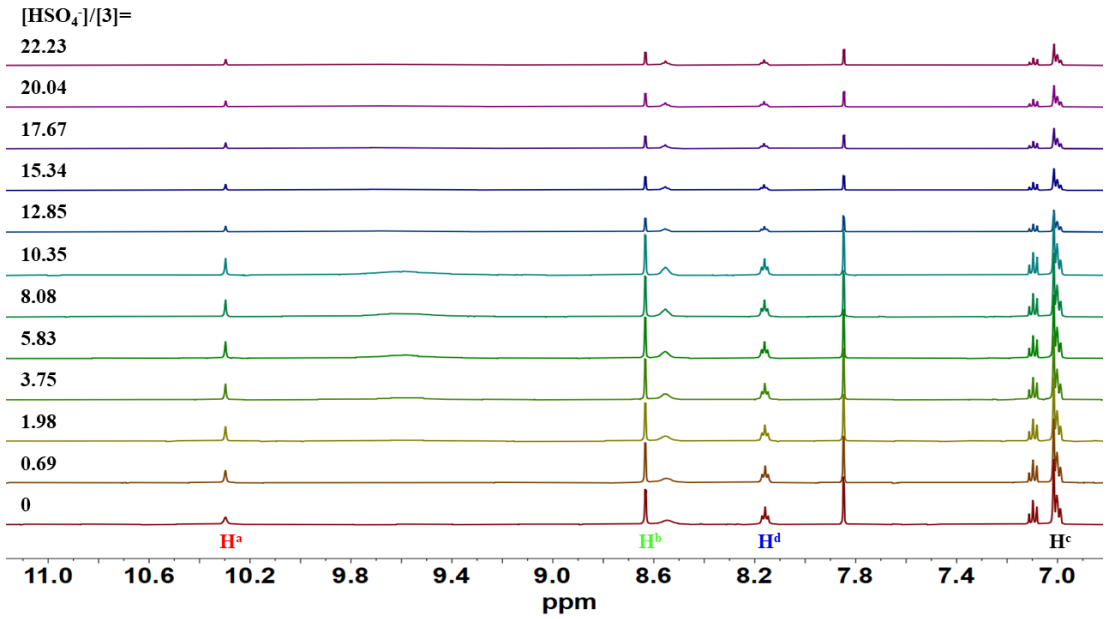

Fig. S32 Stack plot of ^{1}H NMR titration of acyclic receptor **3** (1.0 mM) with ^{n}Bu$_4$NHSO$_4$ in DMSO-d_6 at 298 K.

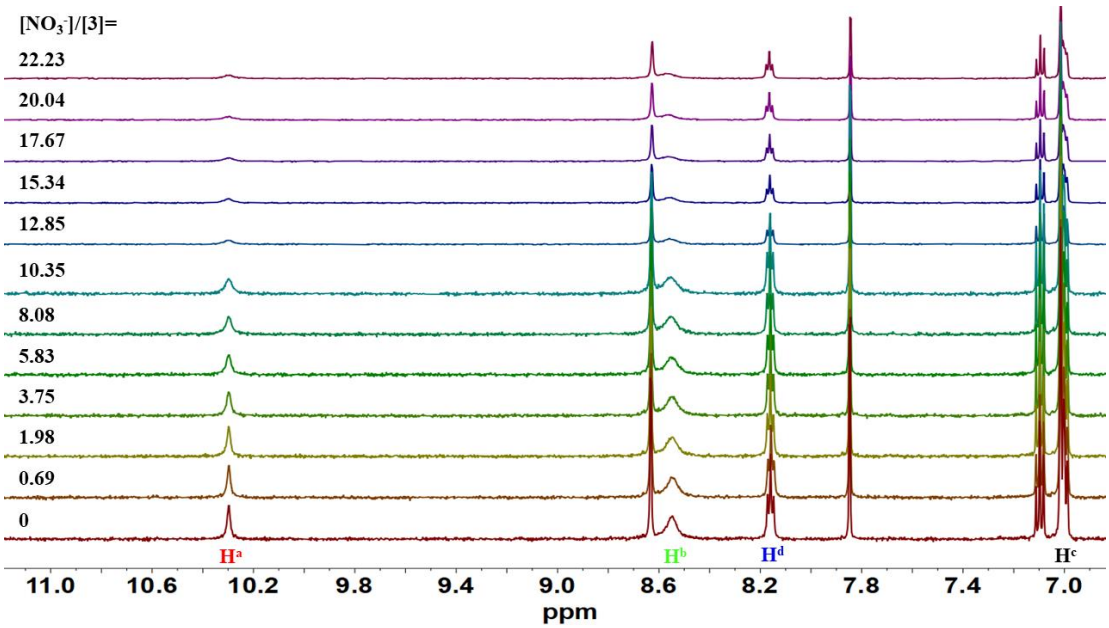

Fig. S33 Stack plot of ^{1}H NMR titration of acyclic receptor **3** (1.0 mM) with $^{n}Bu_4NNO_3$ in DMSO-d_6 at 298 K.

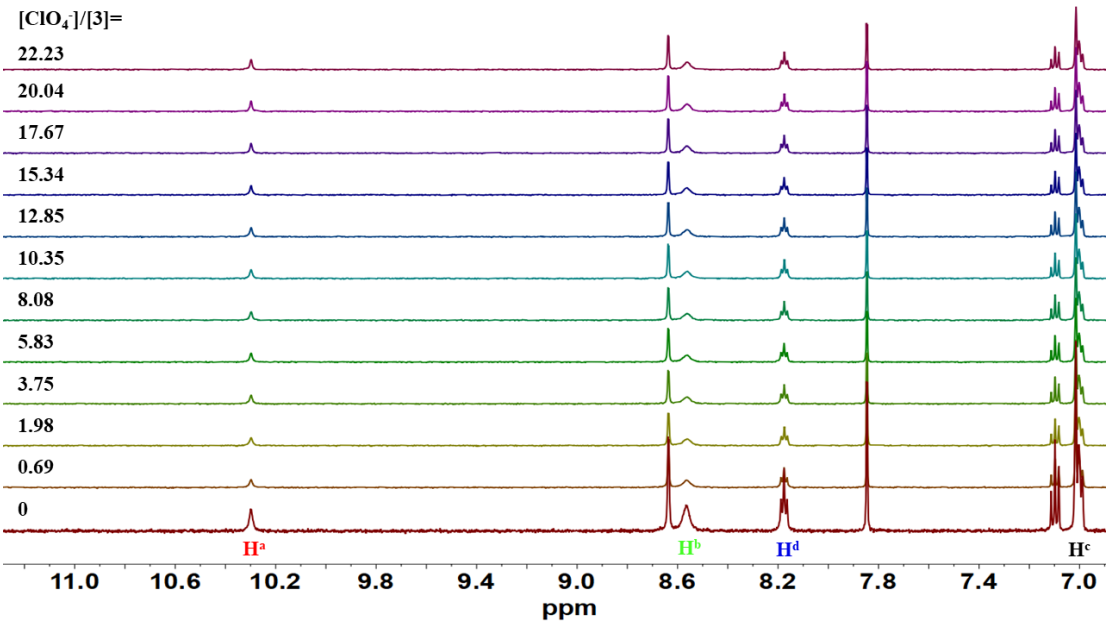

Fig. S34 Stack plot of ^{1}H NMR titration of acyclic receptor **3** (1.0 mM) with $^{n}Bu_4NClO_4$ in DMSO-d_6 at 298 K.

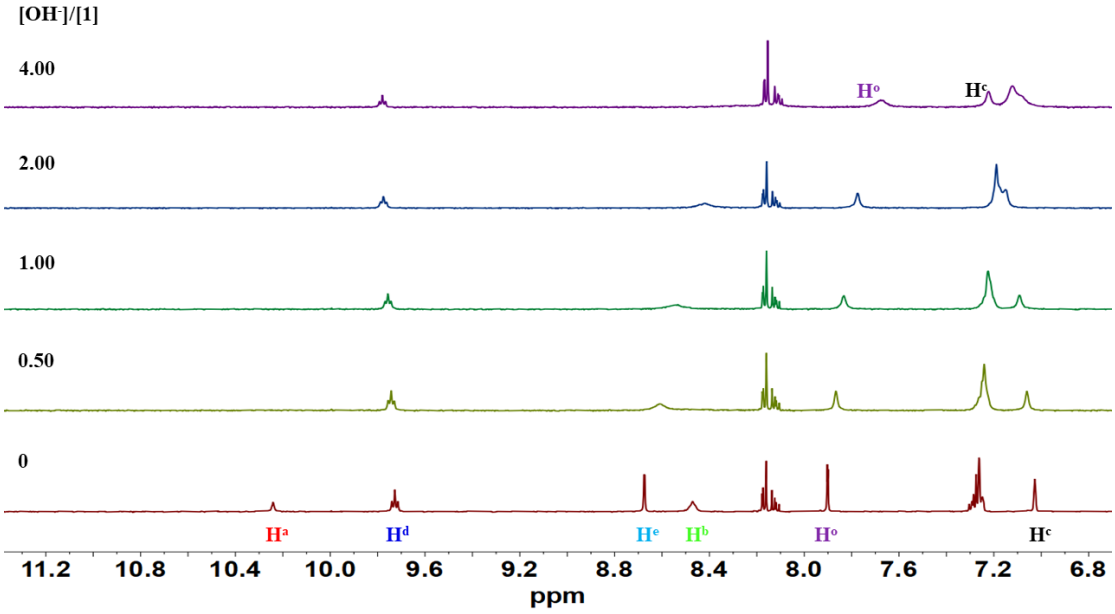

Fig. S35 Stack plot of ^{1}H NMR titration of macrocycle **1** (1.0 mM) with ^{n}Bu$_4$NOH in DMSO-d_6 at 298 K.

UV-vis titrations

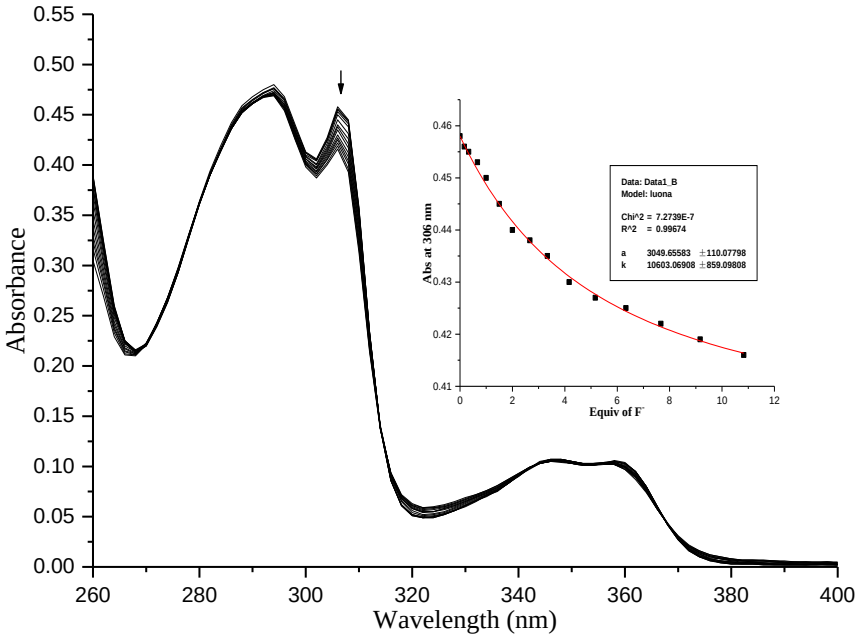

Fig. S36 UV-vis spectral changes of macrocycle **2** (20 μM) upon titration with $^{n}Bu_4NF$ (0~10.8 equiv) in DMSO at 298 K. The inset: The non-linear curve fitting of the absorbance at 306 nm of macrocycle **2** against the added F^-, assuming a 1:1 binding model (K_a = 10603 M^{-1}).

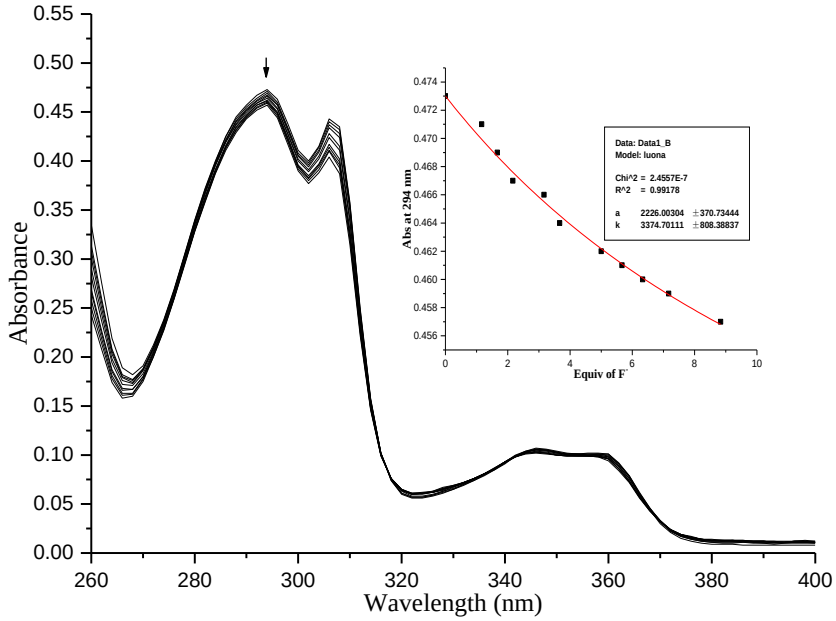

Fig. S37 UV-vis spectral changes of acyclic receptor **3** (20 μM) upon titration with $^{n}Bu_4NF$ (0~8.8 equiv) in DMSO at 298 K. The inset: The non-linear curve fitting of the absorbance at 294 nm of acyclic receptor **3** against the added F^-, assuming a 1:1 binding model (K_a = 3375 M^{-1}).

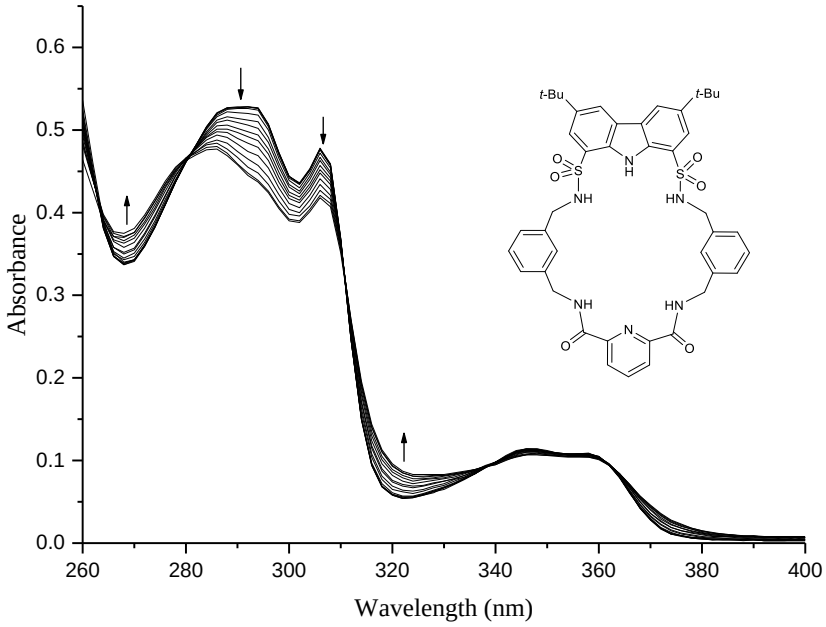

Fig. S38 UV-vis spectral changes of macrocycle **1** (20 μM) upon titration with $^{n}Bu_4NOH$ (0~10.8 equiv) in DMSO at 298 K.

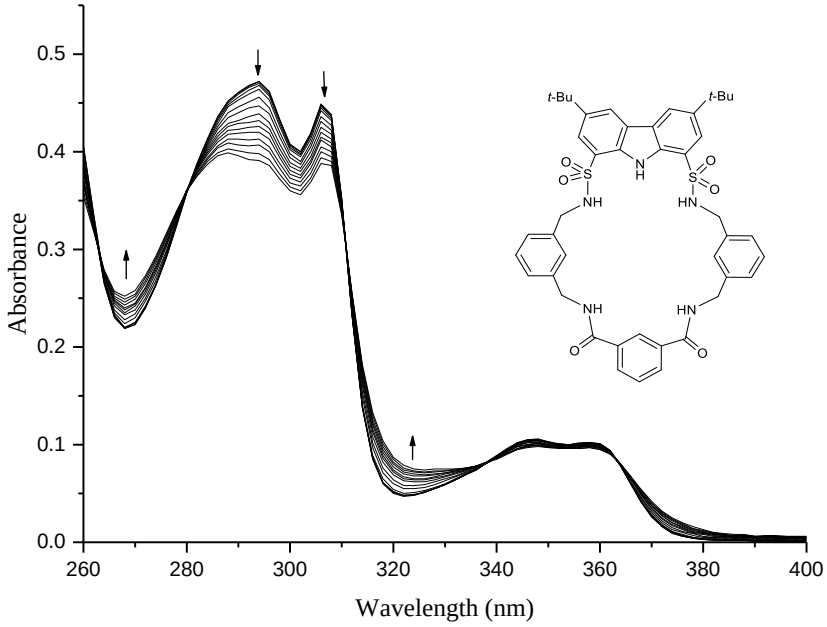

Fig. S39 UV-vis spectral changes of macrocycle **2** (20 μM) upon titration with $^{n}Bu_4NOH$ (0~10.8 equiv) in DMSO at 298 K.

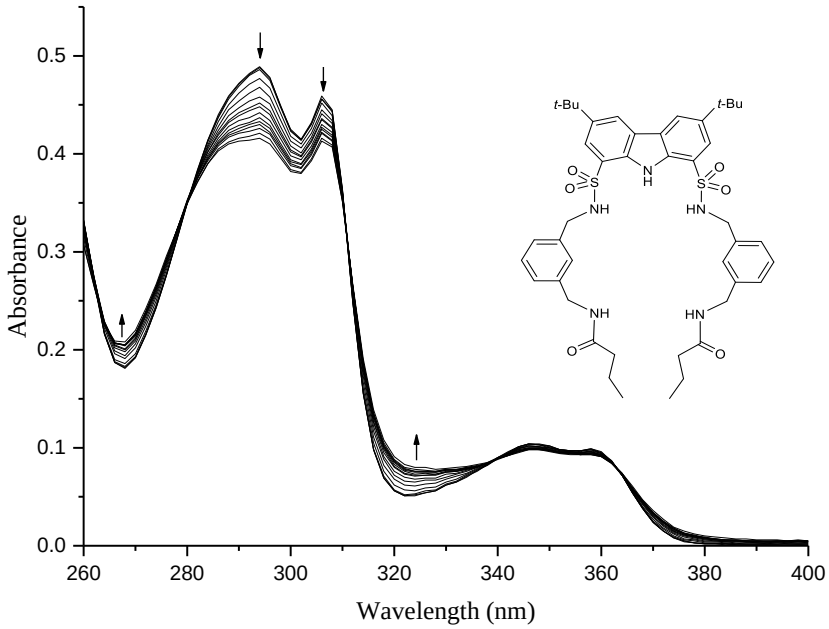

Fig. S40 UV-vis spectral changes of acyclic receptor **3** (20 μM) upon titration with $^{n}Bu_4NOH$ (0~8.8 equiv) in DMSO at 298 K.

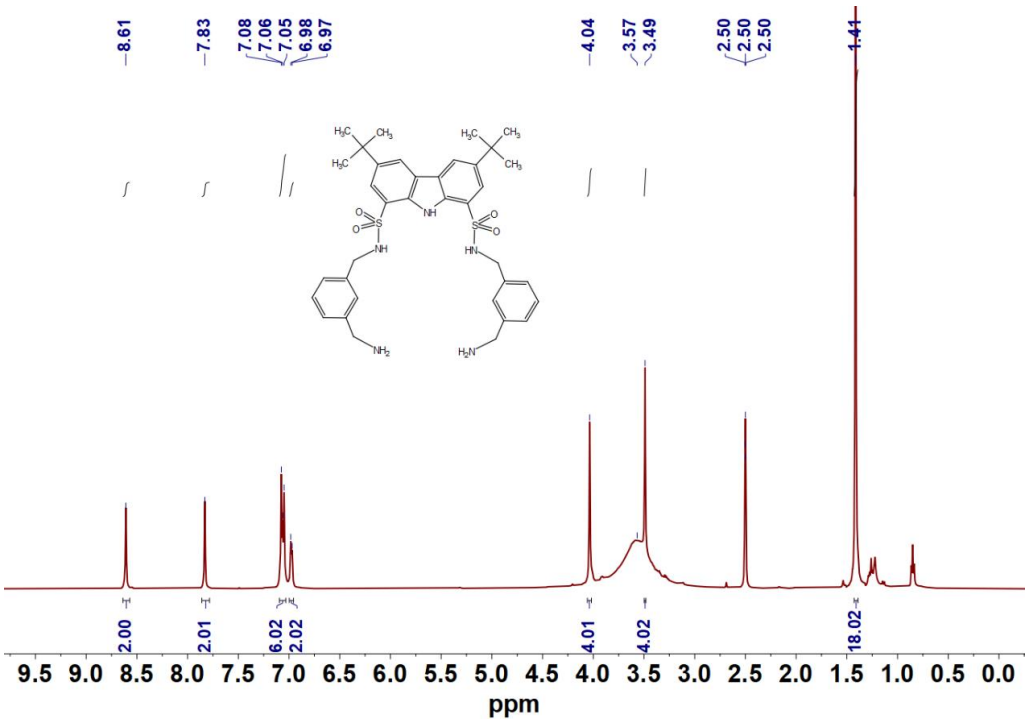

Fig. S41 ^{1}H NMR spectrum of diamine **4** in DMSO-d_6 at 298 K.

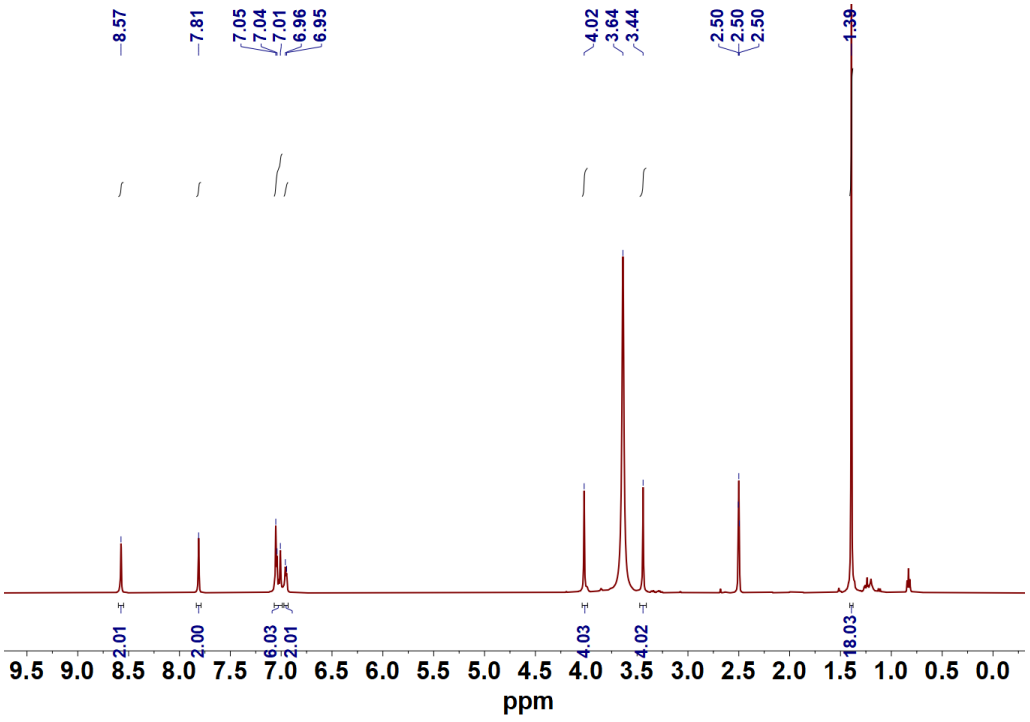

Fig. S42 ^{1}H NMR spectrum of diamine **4** in DMSO-d_6 (D_2O exchange) at 298 K.

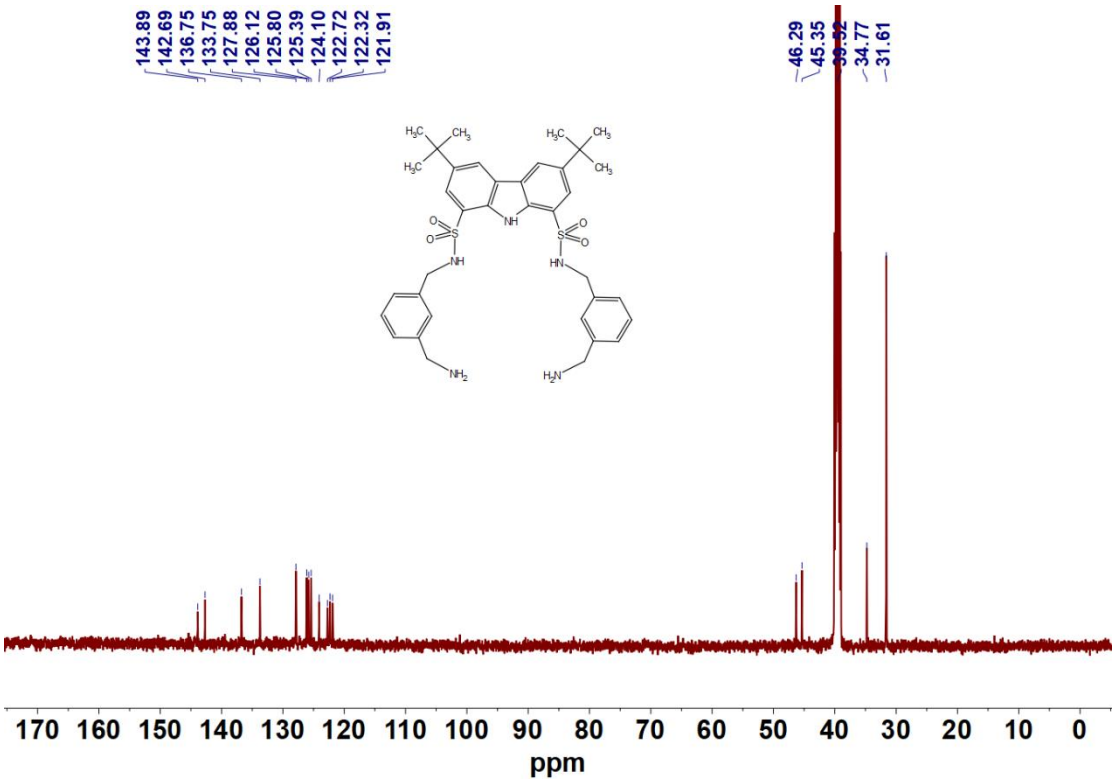

Fig. S43 ^{13}C NMR spectrum of diamine **4** in DMSO-d_6 at 298 K.

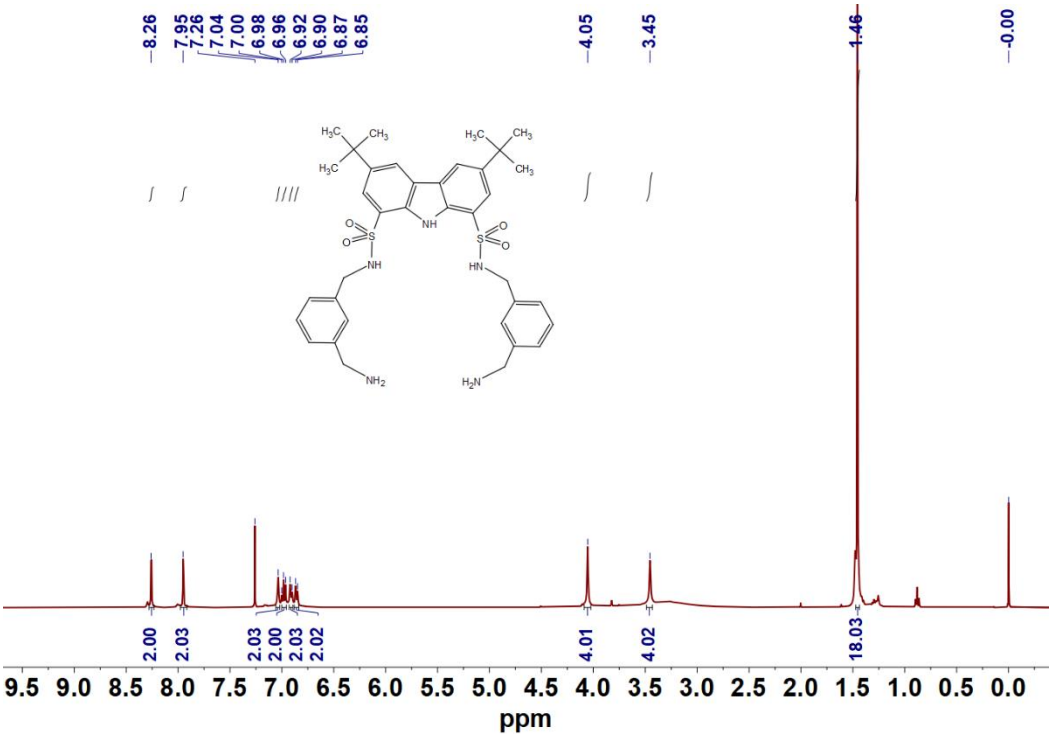

Fig. S44 ^{1}H NMR spectrum of diamine **4** in $CDCl_3$ at 298 K.

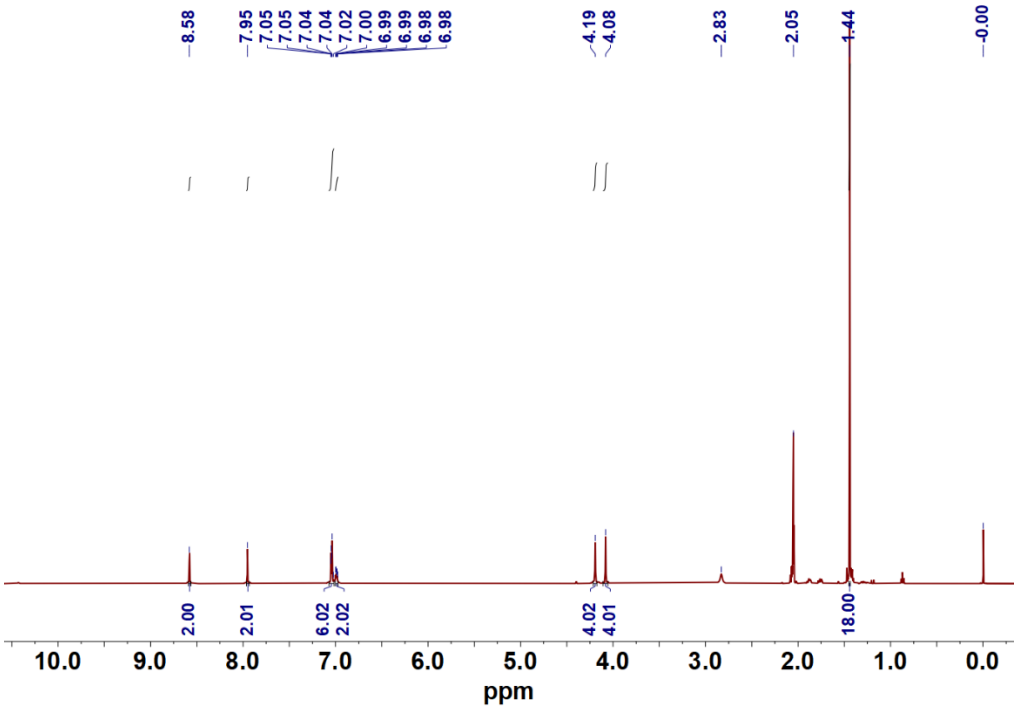

Fig. S45 ^{1}H NMR spectrum of diamine **4** in CD_3COCD_3 at 298 K.

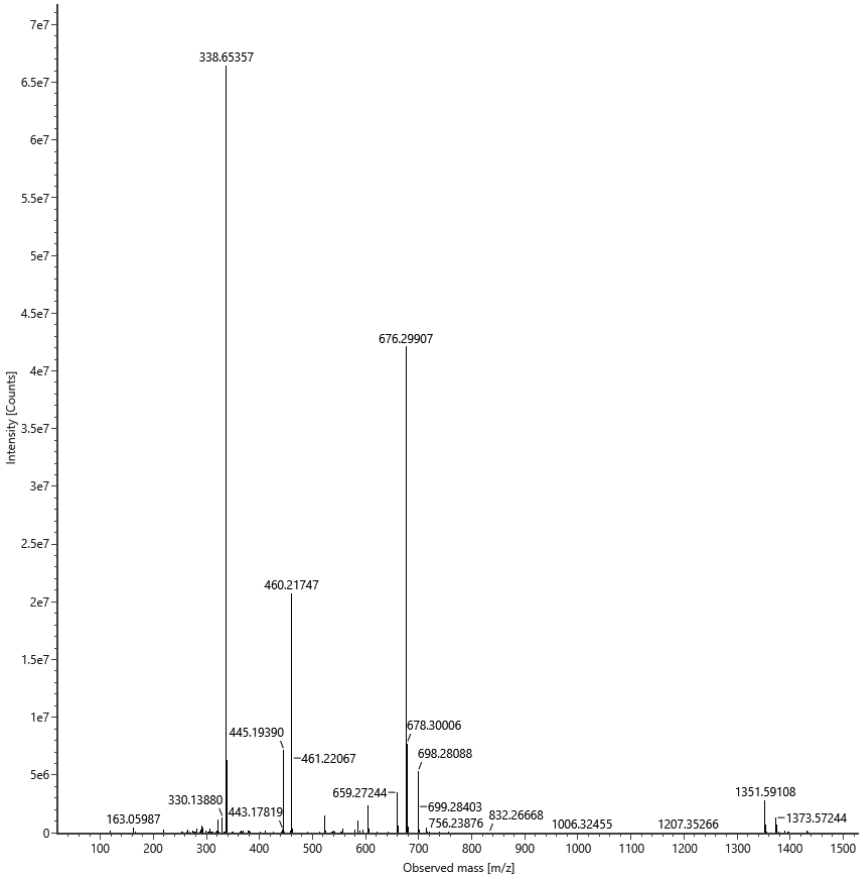

Fig. S46 HRMS-ESI spectrum of diamine **4**.

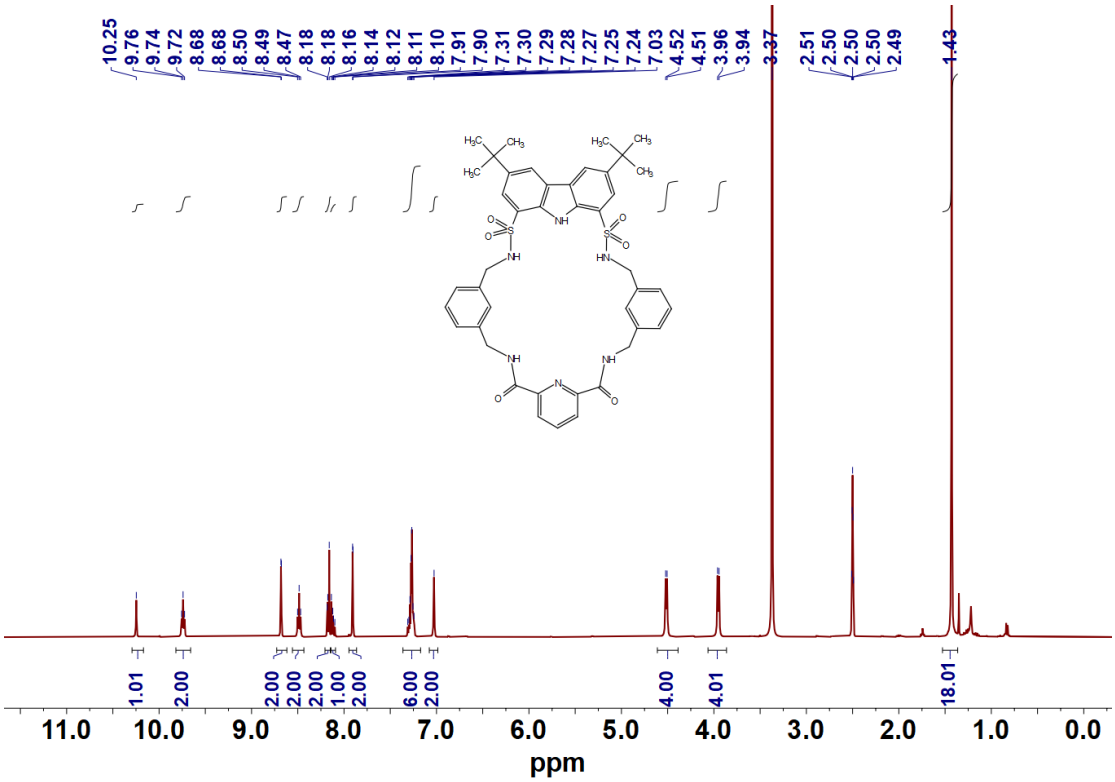

Fig. S47 ^{1}H NMR spectrum of macrocycle **1** in DMSO-d_6 at 298 K.

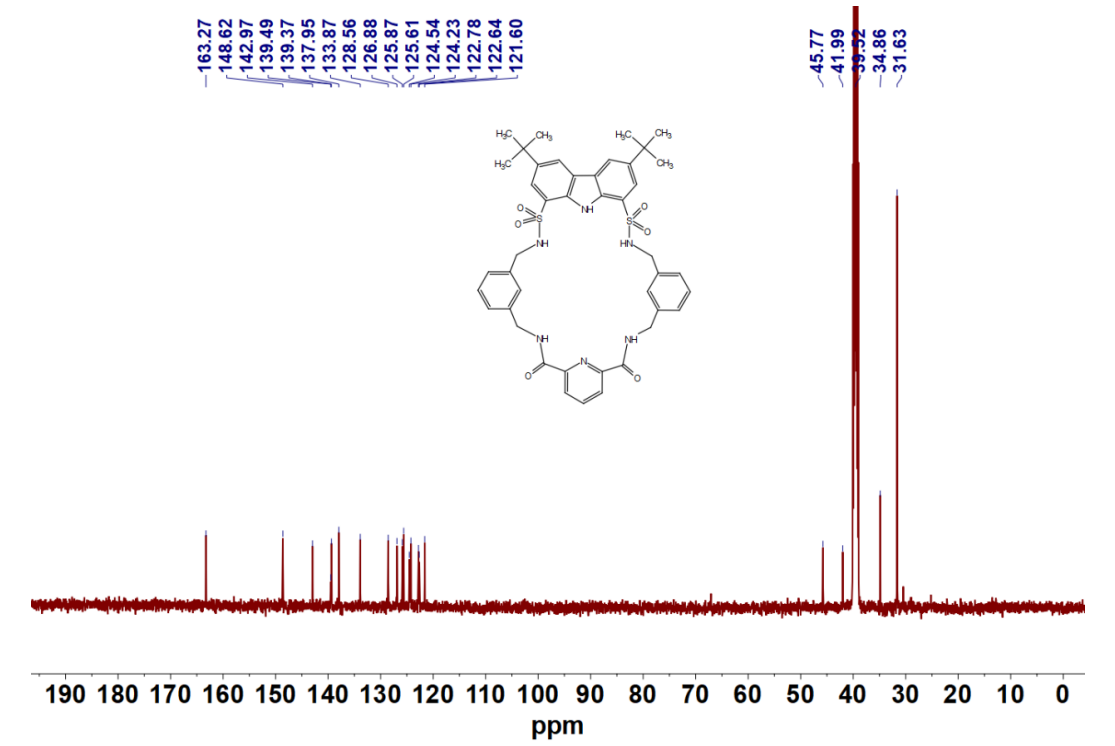

Fig. S48 ^{13}C NMR spectrum of macrocycle **1** in DMSO-d_6 at 298 K.

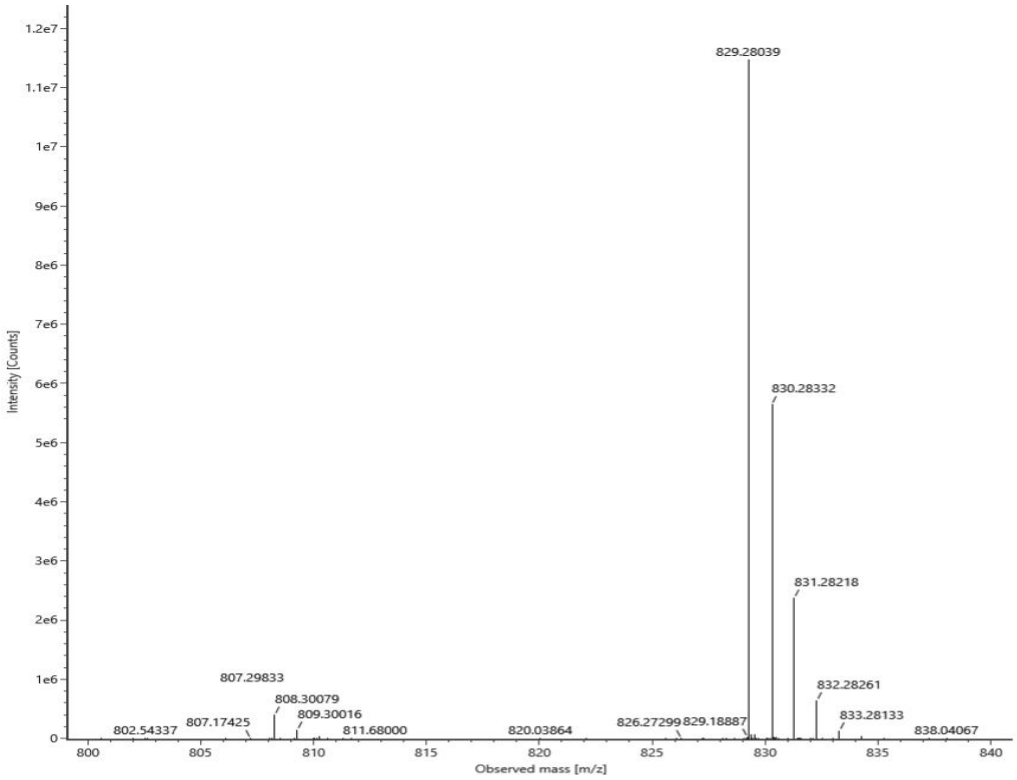

Fig. S49 HRMS-ESI spectrum of macrocycle **1**.

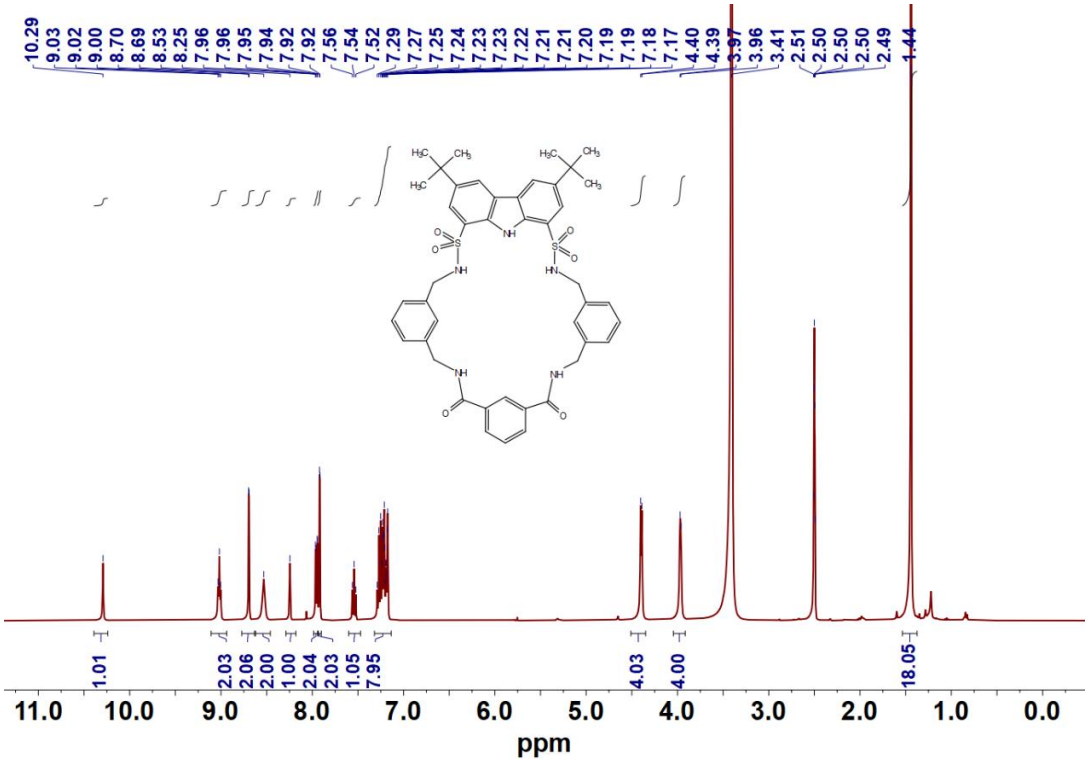

Fig. S50 ^{1}H NMR spectrum of macrocycle **2** in DMSO-d_6 at 298 K.

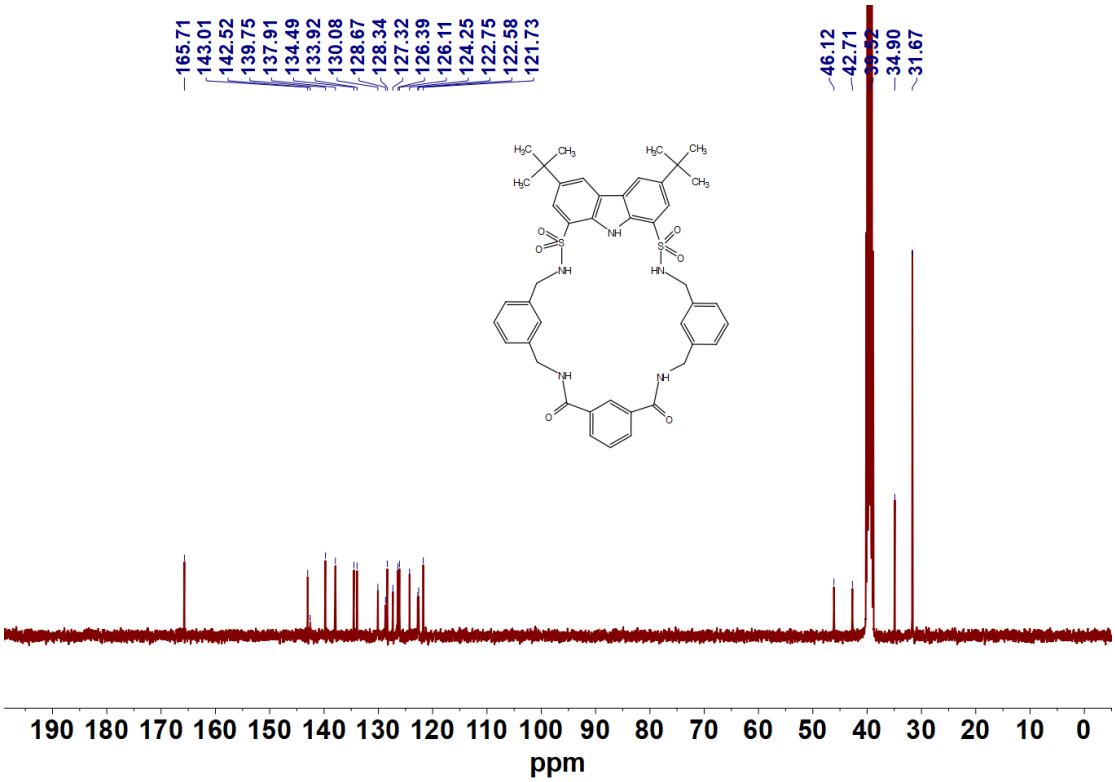

Fig. S51 ^{13}C NMR spectrum of macrocycle **2** in DMSO-d_6 at 298 K.

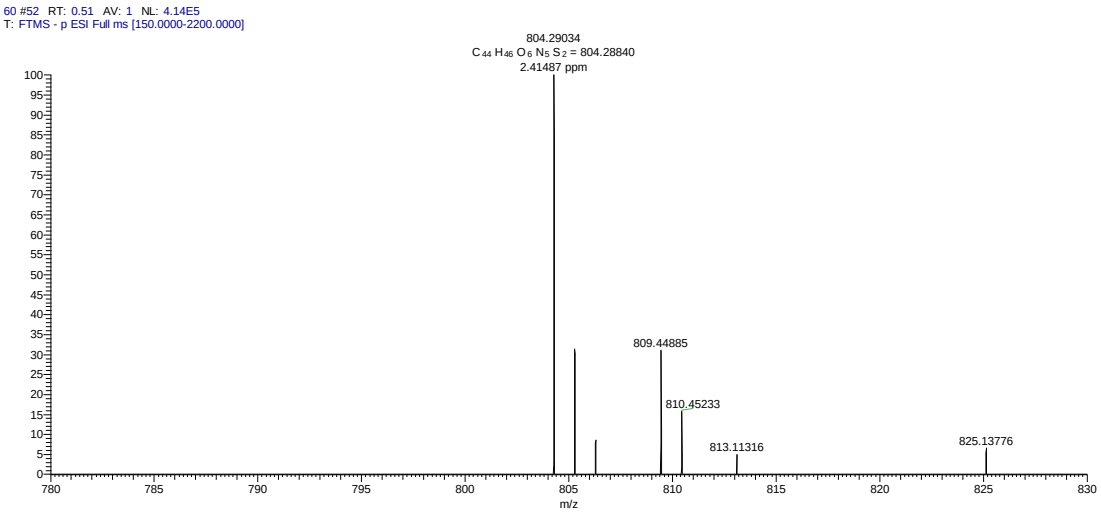

Fig. S52 HRMS-ESI spectrum of macrocycle **2**.

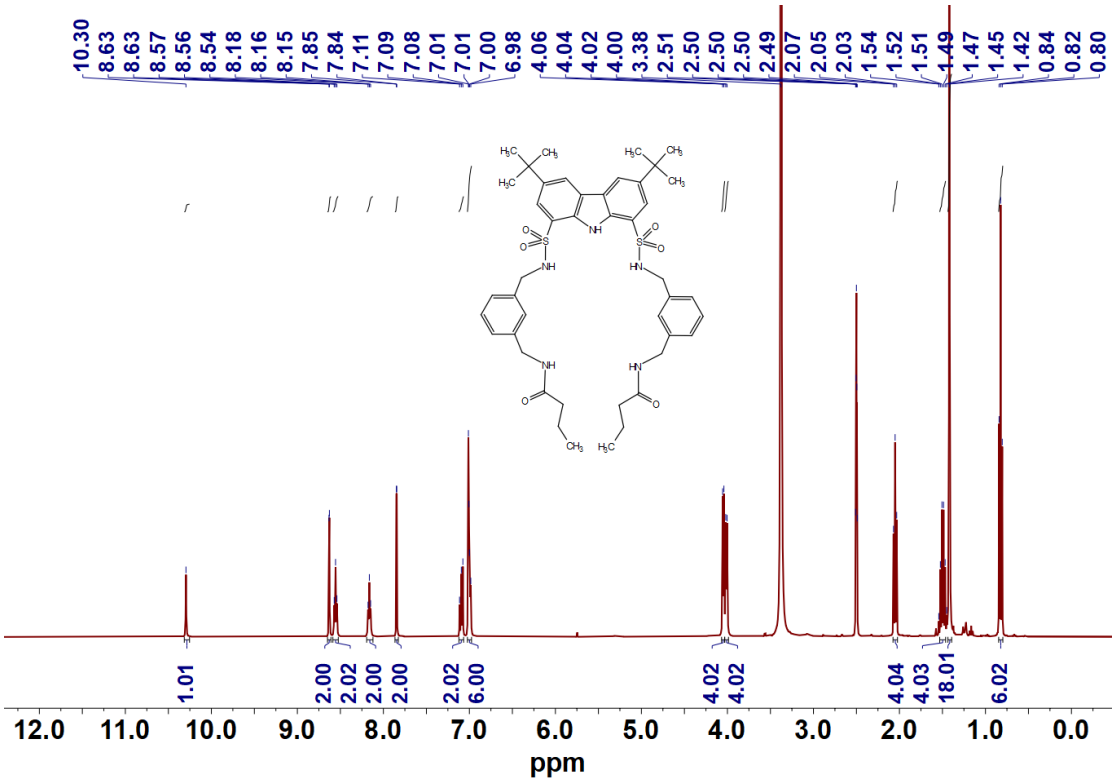

Fig. S53 ^{1}H NMR spectrum of acyclic receptor **3** in DMSO-d_6 at 298 K.

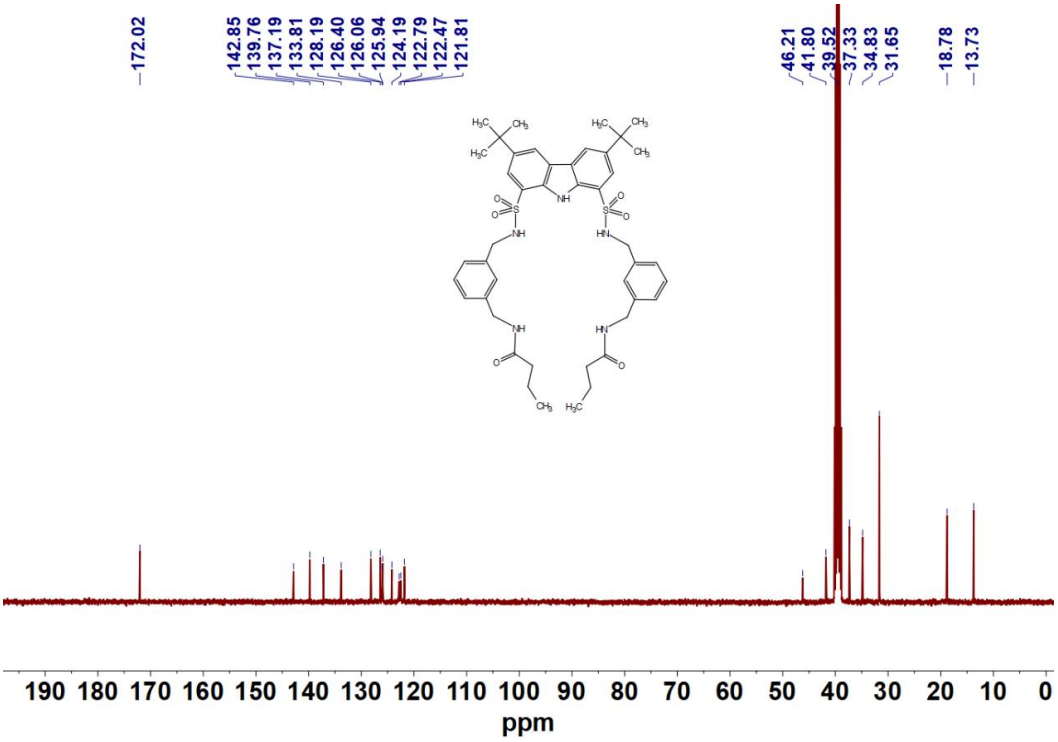

Fig. S54 ^{13}C NMR spectrum of acyclic receptor **3** in DMSO-d_6 at 298 K.

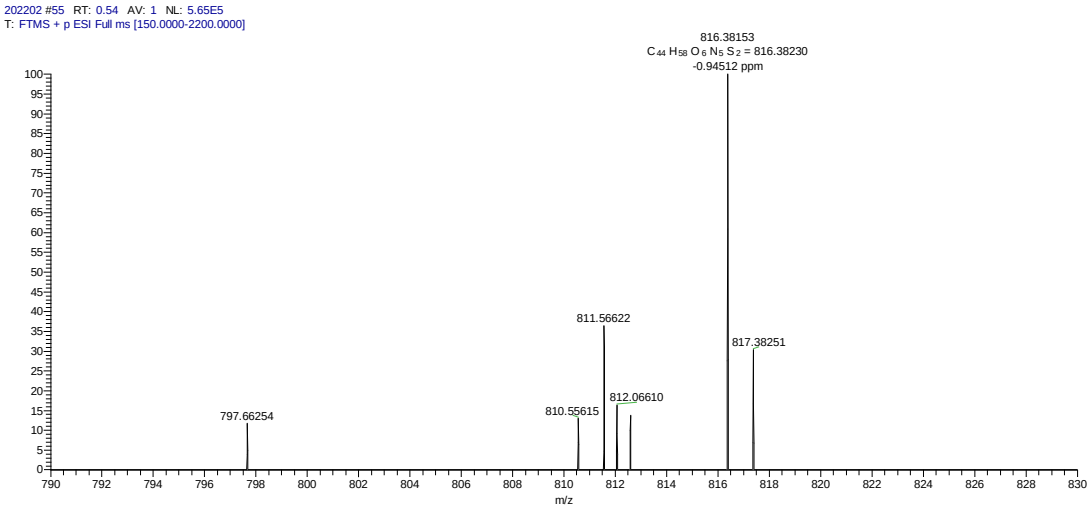

Fig. S55 HRMS-ESI spectrum of acyclic receptor **3**.

X-ray crystallography

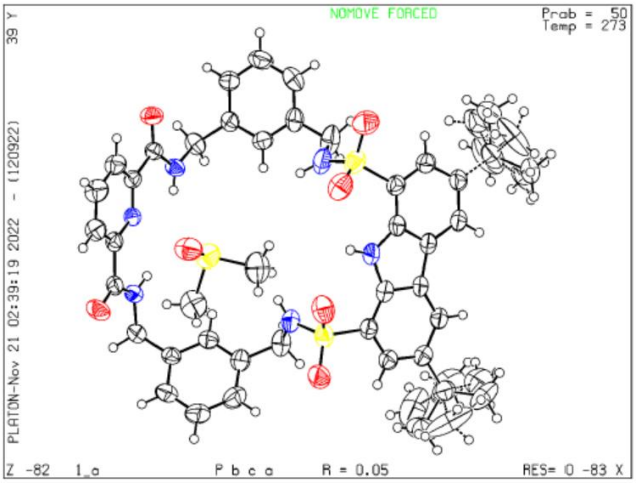

Bond precision: C-C = 0.0038 A Wavelength=0.71073

Cell: a=9.5150(13) b=19.552(3) c=57.266(8)
alpha=90 beta=90 gamma=90

Temperature: 273 K

	Calculated	Reported
Volume	10654(3)	10654(3)
Space group	P b c a	P b c a
Hall group	-P 2ac 2ab	-P 2ac 2ab
Moiety formula	C43 H46 N6 O6 S2, C2 H6 O S [+ solvent]	C43 H46 N6 O6 S2, C2 H6 O S, 2[SOC2H6]
Sum formula	C45 H52 N6 O7 S3 [+ solvent]	C45 H52 N6 O7 S3
Mr	885.11	885.10
Dx,g cm-3	1.104	1.104
Z	8	8
Mu (mm-1)	0.187	0.187
F000	3744.0	3744.0
F000'	3748.46	
h,k,lmax	11,23,68	11,23,68
Nref	9407	9401
Tmin,Tmax	0.967,0.972	0.694,0.746
Tmin'	0.963	

Correction method= # Reported T Limits: Tmin=0.694 Tmax=0.746
AbsCorr = MULTI-SCAN

Data completeness= 0.999 Theta(max)= 25.027

R(reflections)= 0.0533(7650) wR2(reflections)= 0.1455(9401)

S = 1.064 Npar= 634